LoRa Transceiver with Integrated Dual-Band Antenna

Dissertation submitted to
Visvesvaraya National Institute of Technology, Nagpur
In partial fulfillment of the requirements for the award of the degree

Master of Technology
in
VLSI Design

by

Dipshika Khobragade
(MT23MVD019)

Under the guidance of

Prof. Rajendra M. Patrikar

Centre for VLSI and Nanotechnology
Visvesvaraya National Institute of Technology
Nagpur 440010 (India)

June 2025

©Visvesvaraya National Institute of Technology, Nagpur 2025

Centre for VLSI and Nanotechnology
Visvesvaraya National Institute of Technology, Nagpur

DECLARATION

I, **Dipshika Khobragade**, hereby declare that this dissertation titled **"LoRa Transceiver with Integrated Dual-Band Antenna"** is carried out by me in the **Center for VLSI and Nanotechnology** of Visvesvaraya National Institute of Technology, Nagpur. The work is original and has not been submitted earlier whole or in part for the award of any degree/diploma at this or any other Institution / University.

Dipshika Khobragde
Date:

CERTIFICATE

This is to certify that the dissertation titled **"LoRa Transceiver with Integrated Dual-Band Antenna"** is submitted by **Dipshika Khobragade (MT23MVD019)** in partial fulfillment of the requirements for the award of **Master of Technology in VLSI Design,** VNIT Nagpur. The work is comprehensive, complete and fit for final evaluation.

Prof. R. M. Patrikar
Centre for VLSI and Nanotechnology
VNIT, Nagpur.

Prof. Sanjay B. Dhok
Head, Centre for VLSI and Technology
VNIT, Nagpur
Date:_____

Center for VLSI and Nanotechnology
Visvesvaraya National Institute of Technology, Nagpur

June 2025

Date:_____

Non-Plagiarism Certificate

Certified that M. Tech Dissertation titled **"LoRa Transceiver with Integrated Dual-Band Antenna"** submitted by **Dipshika Khobragade (MT23MVD019)** has been checked for plagiarism using TURNITIN software and the overlap is found within prescribed limits. A summary of the report is given below;

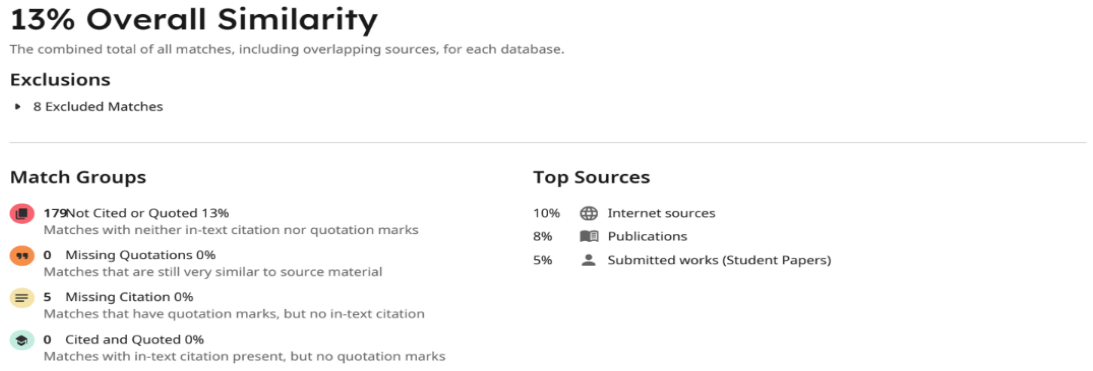
13% Overall Similarity
The combined total of all matches, including overlapping sources, for each database.
Exclusions
8 Excluded Matches
Match Groups
179 Not Cited or Quoted 13%
Matches with neither in-text citation nor quotation marks
0 Missing Quotations 0%
Matches that are still very similar to source material
5 Missing Citation 0%
Matches that have quotation marks, but no in-text citation
0 Cited and Quoted 0%
Matches with in-text citation present, but no quotation marks
Top Sources
10% Internet sources
8% Publications
5% Submitted works (Student Papers)

Figure A: Plagiarism Certificate from Turnitin Software

Dipshika Khobragade
Date:_____

Prof. R. M. Patrikar
Supervisor

Acknowledgement

I would like to start by expressing my gratitude to my supervisor, **Prof. Rajendra M. Patrikar**, for his constant support and encouragement throughout this journey. He gave me the freedom to explore, things. I've learned a lot under his mentorship not just technically, but also, I learned how to approach research with curiosity and discipline.

I would like to thank **Prof. S. B. Dhok**, our Head of Department, for his encouragement in all aspects. I'd like to sincerely thank **Prof. R. B. Deshmukh**, **Dr. G. C. Patil**, **Dr. Vasu Pulijala** and **Dr. Nikhil Deep Gupta** for their valuable input and feedback at various stages of my project. Their suggestions truly helped me to improve the quality of my work.

I would also like to express my sincere regards to **Prof. P. L. Patel**, Director of the Institute; **Prof. V. R. Kalamkar**, Dean (Academics) and **Prof. R. V. Taiwade**, Associate Dean (Academics – PG/PhD), for their support and commitment towards academic environment that empowers students to excel. Their leadership and support in providing the resources and encouragement needed to complete this work.

Finally, I would like to extend my heartfelt thanks to my friends and family. Their unwavering support, words of encouragement, and steady belief in me made a significant difference throughout this journey. In moments of stress or uncertainty, their presence provided the balance and motivation I needed to stay focused and positive.

Dipshika Khobragade

Abstract

As we all know, many of the IoT systems use short-range communication technologies like Wi-Fi, Bluetooth, or Zigbee. These technologies work well for close-range tasks, and they don't work well for long-distance communication, especially in outdoor and remote environments. This limitation is a major challenge in applications, where data needs to travel over several kilometers without draining battery life. Here LoRa (Long Range) technology caters with its ability to offer low-power, long-range communication that's both reliable and cost-effective.

This project mainly revolves around the design of a compact dual-band LoRa transceiver that mainly work for 433 MHz and 870 MHz. The goal was to make the system flexible enough for different regions, also there is a custom-built antenna that can operate at both frequencies, so we don't need multiple antennas.

The antenna was designed, simulated and fabricated. It was then integrated with an SX1276 LoRa module, an ESP32 microcontroller, and an RF switch that lets the system switch between frequencies on demand.

List of Figures

Figure 2.1 Monopole Antenna 9
Figure 2.2 Dipole Antenna 10
Figure 2.3 Helical Antenna 10
Figure 2.4 Meander-line and Inverted F 11
Figure 2.5 Microstrip Patch Antenna 11
Figure 3.1 Up-chirp and Down-chirp 16
Figure 3.2 Spreading Factor Vs Symbol 17
Figure 4.1 LoRa Architecture 22
Figure 4.2 LoRa Frame Format 24
Figure 4.3 LoRa PHY Frame Format 25
Figure 4.4 LoRa MAC Frame Format 27
Figure 5.1 Structure of proposed antenna 33
Figure 5.2 Structure of designed antenna 36
Figure 5.3 Return Loss (S11) vs Frequency Plot 37
Figure 5.4 VSWR vs Frequency Plot 38
Figure 5.5 Z parameter (impedence) vs Frequency Plot 38
Figure 5.6 Y Parameter (Admittance) vs Frequency 39
Figure 5.7 Gain vs Frequency 40 40
Figure 5.8 Radiation Efficiency vs Frequency 40
Figure 5.9 Directivity vs Frequency 41
Figure 5.8 Radiation Pattern 42
Figure 5.11 E-field Distribution at 433MHz and 870MHz 42
Figure 5.12 Current Distribution at 433 MHz and 870 MHz 43
Figure 5.13 2D Radiation Pattern in E-plane and H-plane 44
Figure 5.14 Fabricated antenna 45
Figure 5.15 S11 obtained on VNA 45
Figure 6.1 Block Diagram of Lora Transceiver 47
Figure 6.2 SX1276 Lora Transceiver Module 50
Figure 6.3 ESP32 and SX1276 interfacing diagram 52

Figure 6.4 PE4259 RF Switch in Transceiver system 54
Figure 6.5 Schematic Diagram for LoRa system 57
Figure 6.6 Antenna Switching flow chart using ESP32 and PE4259 57
Figure 6.7 Top Layer and Bottom Layer Routing 59
Figure 6.8 1st inner layer ad 2nd inner layer Routing 59

List of Tables

Table 1.1. Comparison of Wireless Communication Technologies 3

Table 3.1. ISM Bands 15

Table 3.2. Impact of Bandwidth on LoRa Communication 19

Table 5.1. Comparisons of Antenna Types for LoRa Applications 31

Table 5.2. Dimensions of The Proposed Antenna Design 33

Table 6.1. SX1276 LoRa Transceiver Module Pim Description 49

Table 6.2. Pin Mapping Between ESP32 and SX1276 52

Table 6.3. Pin Mapping Between ESP32, SX1276 and PE4259 54

Abbreviations

IoT	Internet of Things
LoRa	Long Range
PCB	Printed Circuit Board
RF	Radio Frequency
CSS	Chirp Spread Spectrum
LoRaWAN	LoRa Wide Area Network
ISM	Industrial, Scientific, and Medical (Bands)
MPA	Microstrip Patch Antenna
FSK	Frequency Shift Keying
ASK	Amplitude Shift Keying
SF	Spreading Factor
ADR	Adaptive Data Rate
ToA	Time on Air
PHY	Physical Layer
MAC	Medium Access Control Layer
CRC	Cyclic Redundancy Check
FHDR	Frame Header
FRMPayload	Frame Payload
MIC	Message Integrity Code
DevAddr	Device Address
FCtrl	Frame Control
AppSKey	Application Session Key
HFSS	High Frequency Structure Simulator
VSWR	Voltage Standing Wave Ratio
VNA	Vector Network Analyzer

Index

Abstract ..... **i**

List of Figures ..... **ii**

List of Tables ..... **iv**

Abbreviations ..... **v**

Chapter 1: Introduction

1.1 Background 2
1.2 Motivation 3
1.3 Thesis Organization 5

Chapter 2: Literature Review

2.1 LoRa Technology for Internet of Things (IoT) 7
2.2 Antennas for LoRa-Based IoT Applications 8
2.3 Types of Antennas 9
2.3.1 Monopole Antennas 9
2.3.2 Dipole Antennas 9
2.3.3 Helical Antenna 10
2.3.4 Meander-Line and inverted F 11
2.3.5 Microstrip Patch Antenna 11
2.4 Types of Frequency Bands in LoRa Antenna Design 12
2.4.1 Single Band Antennas 12
2.4.2 Dual Band Antennas 12
2.4.3 Multiband Antennas 12

Chapter 3: Lora Technology

3.1 Overview of LoRa Technology 14
3.2 Industrial, Scientific, and Medical (ISM) Bands 15

3.3 LoRa Modulation Scheme 16
3.3.1 Chirp Spread Spectrum (CSS) 16
3.3.2 Spreading Factor 17
3.3.3 Bandwidth 18
3.3.4 Symbol Modulation and mathematical model 19
3.3.5 Dechriping and Demodulation Technique 20

Chapter 4: LoRa Network Architecture

4.1 Overview of LoRa Architecture 22
4.2 LoRa Frame Format 23
4.3 LoRa PHY Layer 25
4.4 LoRa MAC Layer 26
4.5 LoRa Application Layer 28

Chapter 5: Design of Dual Band Microstrip Patch Antenna

5.1 Introduction 30
5.2 Antenna Design Specifications 32
5.3 Design Methodology 34
5.4 Simulation Setup 35
5.5 Simulation Results and Analysis 37
5.6 Fabrication and Testing 44

Chapter 6: LoRa Transceiver System Integration

6.1 Overview of LoRa Transceiver Module SX1276 48
6.2 Interfacing with ESP32 51
6.3 Role and Configuration of RF Switch 53
6.4 Antenna Port Switching Logic 55
6.5 PCB Design 58

Chapter 7: Conclusion and Future Scope

7.1 Conclusion… 61
7.2 Future Scope 61

8 References **62**

1

INTRODUCTION

1.1 Background

The Internet of Things (IoT) is becoming an essential part of our everyday lives. Whether it's smart home devices that make life more convenient, or sensors used in agriculture to monitor soil and weather conditions, IoT technology is helping us build smarter, more connected systems. At the heart of all these applications is the need to share data wirelessly and that's where some challenges begin. Most commonly used wireless technologies like Wi-Fi, Bluetooth, and Zigbee work well for short distances, but they're not ideal when you need to send data over longer ranges or when power supply is limited.

That's where LoRa (Long Range) comes into play. LoRa is built specifically for long-distance communication while keeping power usage extremely low. It works on sub-GHz frequencies and uses a special modulation technique (called chirp spread spectrum) that lets it send data over long distances—even through trees, buildings, or other interference. It's ideal for battery-powered devices that need to work reliably for a year or more without needing attention.

But most LoRa modules today are designed to work on just one frequency band. This becomes a problem because different countries use different frequency ranges for LoRa communication. That's why this project focuses on designing a dual-band LoRa transceiver that works on both 433 MHz and 870 MHz, making it more flexible and practical for real-world applications.

This work aims to build a compact system with a custom antenna and smooth frequency switching, so IoT devices can adapt to a wider range of environments and regulations.

1.2 Motivation

My journey into wireless communication and IoT was sparked by a desire to contribute something meaningful to the growing world of smart technology. As our systems grow more connected, efficient communication becomes not just a luxury but a necessity especially in rural, industrial, and environmental settings where infrastructure is limited, and energy needs to be conserved. This led me to explore alternative communication technologies that could overcome these limitations. Among the various options available, LoRa stood out for its impressive range and ultra-low power consumption. The following table compares common wireless technologies used in IoT and highlights why LoRa offers a unique advantage in rural and remote applications.

Technology	Frequency Band	Range	Power Consumption	Data Rate	Use Cases
Wi-Fi	2.4 GHz / 5 GHz	~50–100 meters	High	High (10s–100s Mbps)	Smart homes, video streaming
Bluetooth	2.4 GHz	~10–30 meters	Medium	Medium (~1 Mbps)	Wearables, short-range sensors
Zigbee	2.4 GHz	~10–100 meters	Low	Low (~250 kbps)	Home automation, industrial monitoring
LoRa	433 MHz / 868 MHz / 915 MHz	**Up to 15 km (rural)**	**Very Low**	Low (~50 kbps)	Agriculture, smart cities, remote sensing
NB-IoT	Licensed LTE Bands	~10 km (urban)	Low	Medium (~100 kbps)	Smart metering, asset tracking

Table 1.1: Comparison of Wireless Communication Technologies

Technologies like Wi-Fi, Bluetooth, and Zigbee serve us well in urban and short-range scenarios, but they fall short when tasked with covering large geographical areas or operating in remote locations. This is where LoRa (Long Range) technology stands out. It's purpose-built for long-distance, low-power communication, which makes it ideal for IoT devices operating in remote or off-grid locations. But as I dug deeper into LoRa systems, I found a recurring limitation that caught my attention most LoRa modules are restricted to a single frequency band. While that works fine in controlled or localized settings, it becomes a significant challenge if you want to build devices that can work in different countries or environments where frequency regulations vary.

What really sparked this project was a simple but powerful realization: most LoRa devices are limited to a single frequency band and that just doesn't cut it for today's global, interconnected world. I wanted to create something more flexible. So, I set out to design a LoRa transceiver that could operate on both 433 MHz and 870 MHz, two widely used frequency bands. With that flexibility, one piece of hardware could be used in different regions without having to start from scratch every time. It's about making development easier, smarter, and ready to scale.

So, I focused on a design that's compact, adaptable, and future-ready. By combining dual-band operation with seamless switching between frequencies, my goal is to help enable IoT systems that aren't just technically sound, but truly practical. I want this project to contribute to a future where smart technology can go farther literally and figuratively reaching places and solving problems where it couldn't before.

1.3 Thesis Organization

This research study thesis contains the following 6 chapters as discussed below.

Chapter 1:

Introduces the project, provides background information, motivation for starting the project and describes the structure of the thesis.

Chapter 2:

This chapter provides a comprehensive literature review. It discusses the role of LoRa for IoT, covering antenna designs, antenna types, and commonly used frequency bands in LoRa communication.

Chapter 3:

In this chapter, we explore the basic ideas and important features that make LoRa technology unique and useful. It explains the working of LoRa modulation, the usage of ISM bands, and how Chirp Spread Spectrum (CSS) enhances range and robustness in wireless environments.

Chapter4:

This section outlines the structural components and operational flow of a standard LoRa network. It elaborates on the LoRa PHY and MAC layers, the structure of a LoRa frame, and the overall communication stack, culminating in the application layer used by end devices.

Chapter5:

This chapter outlines the design and simulation of a dual-band microstrip patch antenna targeting 433 MHz and 870 MHz, including specifications, methodology, and analysis of return loss and impedance using HFSS.

Chapter6:

This chapter presents the conclusion and future work.

2

LITERATURE REVIEW

2.1 LoRa Technology for Internet of Things (IoT)

LoRa technology is designed for long-range communication with minimum energy consumption making it convenient for long range Internet of Things (IoT) applications. LoRa uses Chirp Spread Spectrum (CSS) modulation, which allows signals to travel over long distances. It operates on unlicensed frequency bands i.e. ISM band, enabling cost-effective deployment without licensing fees.

LoRa has a ability to balance range and data rate through spreading factor. As described by Bor, Vidler, and Roedig, by increasing the spreading factor we can also increase the communication range. [1].

LoRa's power consumption is very low, making it suitable for battery-powered IoT devices expected to operate for years without maintenance. Adelantado et al. observed that devices using LoRa can function on standard coin-cell batteries for up to 10 years, depending on transmission frequency.[2].

Another advantage of LoRa is that uses unlicensed ISM bands which allows for cost-free deployments across different countries. Research by Centenaro, Vangelista et al. highlights how this regional adaptability helps to scale IoT networks without any complex regulatory approvals [3].

2.2 Antennas for LoRa-Based IoT Applications

In a LoRa based IoT devices, the antenna is a critical component that directly impacts communication range, power efficiency, and reliability. As LoRa is built for long-range, low-power communication, the antenna must be carefully designed to match these goals. According to Ranaweera and Jayasundara, an optimized antenna can enhance LoRa coverage without increasing the transmission power, hence preserving battery life [4].

LoRa devices works with sub-GHz frequency bands like 433 MHz, 868 MHz, or 915 MHz, depending on the region they are used. Antennas designed for these bands should have strong impedance matching, high radiation efficiency, and compact size suitable for embedded applications. In research by Bouchouicha et al., a monopole antenna was developed for the 868 MHz and he achieved a communication range of 10 km with minimum energy consumption [5].

Integrating these antennas into real-world LoRa devices comes with challenges such as Size constraints, environmental factors, and device orientation can all impact performance. Researchers like Nguyen et al. developed a 433 MHz meander-line antenna that was both omnidirectional achieving excellent coverage while maintaining the low-profile needed for sensor nodes.[6].

For devices to work across multiple frequency bands dual-band antennas are increasingly being researched. M. A. Islam et al. proposed a dual-band printed monopole antenna that operate across two frequencies 433 MHz and 915 MHz. This design used a combination of T-shaped slots and stepped ground planes to achieve both frequencies with low return loss and gain [7].

Antenna placement and material choice and plays an important role. LoRa antennas are often mounted on PCBs, which can detune the antenna or absorb radiated power. S. Rajendran et al. explored ceramic-based chip antennas for LoRa nodes, offering durability and consistent performance [8].

2.3 Types of Antennas

In LoRa communication, the antenna is a main component that influences the overall performance and reliability of the network. It directly affects parameters such as signal strength, range, and energy efficiency. Since LoRa operates in sub-GHz bands, antennas must be carefully chosen to get the required frequency and device size. Below is the breakdown of the most common antenna types used for LoRa applications:

2.3.1 Monopole Antennas

Monopole antennas are mostly used in LoRa applications. They consist of a single radiating element and require a ground plane to function efficiently. These antennas are easy to integrate and design, especially when printed directly on the PCB.

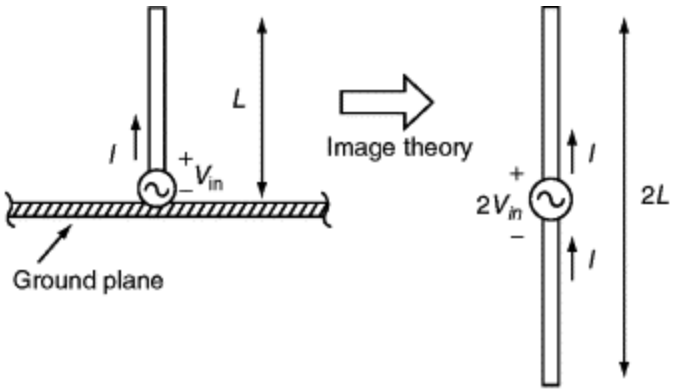

Figure 2.1 Monopole Antenna

2.3.2 Dipole Antennas

Dipole antennas consist of two conductive arms and offer balanced signal transmission and reception. Because of its symmetrical design, it tends to perform better than monopoles especially outdoors. Dipoles are a solid choice when you need stable connectivity in all directions.

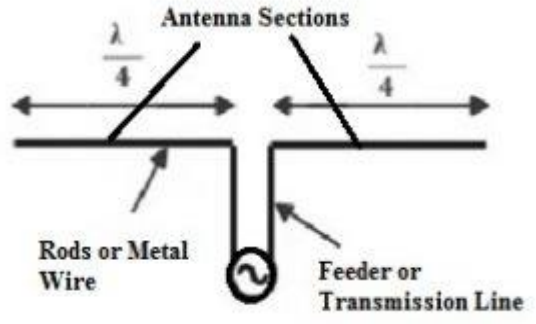

Figure 2.2 Dipole Antenna

2.3.3 Helical Antennas

Helical antennas are formed by winding a conductive wire into a spring-like shape, which gives high radiation and compact size. This helps helical antennas to compact by still offering strong signal performance. These are used for applications where space is limited but a long range is required, and hence making it useful for portable LoRa devices.

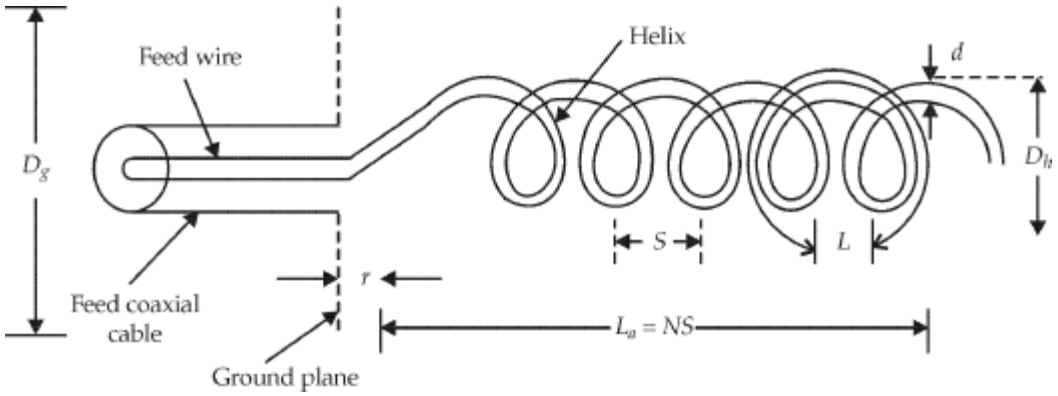

Figure 2.3 Helical Antenna

2.3.4 Meander-Line and Inverted-F Antennas

Meander-line antennas use zigzag pattern to increase the current path length without increasing the physical size of the antenna. This allows the antenna to resonate effectively at lower frequencies. They are ideal for embedded IoT sensors where compactness is required.

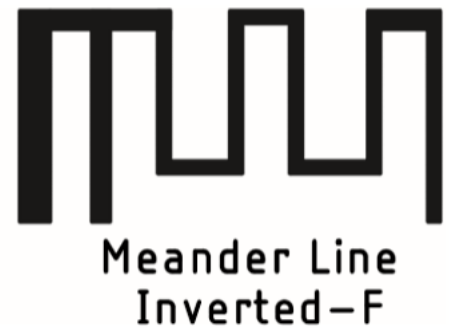

Figure 2.4 Meander-line and Inverted-F

2.3.5 Microstrip Patch Antennas

Microstrip Patch Antennas (MPAs) offer the best of both worlds. They are compact and are capable of delivering high gain, making them ideal for directional communication. Their planar design allows PCB integration efficiently. MPAs can be tuned to operate at LoRa specific bands like ensuring optimized performance.

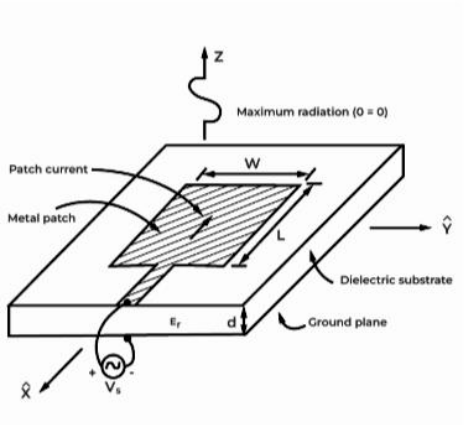

Figure 2.5 Microstrip Patch Antennas

2.4 Types of Frequency Bands in LoRa Antenna Design

In LoRa based IoT systems, the antenna's operating frequency band is a crucial design parameter. Depending on the application and regional requirements, antennas are mainly categorized into three major configurations single-band, dual-band and multi-band. Each type of configuration offers trade-offs in terms of bandwidth, size, complexity, and versatility.

2.4.1 Single-Band Antennas

Single-band antennas operate at one resonant frequency commonly 433 MHz, 868 MHz, or 915 MHz for LoRa applications. These antennas are simple to design and manufactured, for providing good efficiency and narrowband performance due to excellent impedance and focused current distribution. They are ideal for devices in regions where frequency flexibility is not needed [9].

2.4.2 Dual-Band Antennas

Dual band antennas resonate at two different frequencies. This allows devices to switch between, the different range of frequency by improving coverage and adaptability. These antennas achieve dual resonances by adding slots or parasitic elements, which alter current paths to support dual resonant modes. A notable implementation achieved dual-band operation by etching slots into a microstrip patch, enabling operation at both 433 MHz and 868 MHz while maintaining compact size and low return loss [10].

2.4.2 Multi-Band Antennas

Multi-band antennas operate over three or more frequency bands. These are particularly mostly used in hybrid IoT devices that combine LoRa with other protocols such as Wi-Fi or Zigbee. Multi-band behavior is achieved by techniques like meander-line structuring. While these designs allow seamless communication across different standards without requiring separate antennas, enhancing integration. [11].

3

LoRa TECHNOLOGY

3.1 Overview of LoRa Technology

LoRa is a wireless communication technology used for low power consumption, extended communication range, and high data rate. It is mainly used for IoT devices that can operate in remote areas where battery replacement is difficulty and the data is to be communicated over several kilometers by utilizing minimum power. Also, Lora allows signals to travel over long range when compared with other wireless technologies.

LoRa has ability to operate in unlicensed ISM bands, making it cost effective for a wide range of applications. These frequencies offer, signals to travel over long distances with low signal attenuation and low power consumption especially at sub GHz levels.

When using wireless technology for long-distance communication, power consumption and communication range are frequently traded off. Higher power is typically needed; However power conservation can occasionally result in a shorter transmission distance for data. By using chirp spread spectrum modulation instead of traditional Amplitude Shift Keying or Frequency Shift Keying, LoRa enhances communication range while maintaining low power usage. This allows devices to transmit data over several kilometers on minimum energy, making it ideal for battery powered IoT deployment.

LoRa is most often combined with the LoRaWAN protocol, which handles the network layer and guarantees a scalable, secure, and bidirectional communication between devices. The LoRaWAN architecture follows a star-of-stars topologyin this individual end devices communicate wirelessly with adjacent gateways, which in turn forward the data to a central server. This setup allows for well-organized coordination of a large number of devices across varied geographic areas, making it ideal for IoT applications. This approach reduces energy consumption at the node level and allows the infrastructure to scale proficiently.

3.2 Industrial, Scientific, and Medical (ISM) Bands

The ISM (Industrial, Scientific, and Medical) bands discuss to specific portions of the radio frequency (RF) spectrum kept internationally for non-commercial use. Originally chosen to tackle applications like microwave ovens and medical diathermy devices, these bands are now widely used for wireless communication technologies, including Wi-Fi, Bluetooth, LoRa and Zigbee.

As we all know ISM bands are license free thus, we can use them to install wireless devices without seeking the government permissions, provided that they agree to local regulations like duty cycles and power constraints.

Region	ISM Band Frequency
Europe	433 MHz, 868 MHz
North America	902–928 MHz
Asia	433 MHz, 920–925 MHz
India	865–867 MHz
Australia	915–928 MHz

Table 3.1: - ISM BANDS

These frequencies come under the sub-GHz spectrum, which is vital for long-range, low-power communication. Signals at these lower frequencies have better propagation, allowing them to travel further distances and penetrate obstacles like walls and trees better than signals at higher frequencies.

Because of their varied availability and favorable characteristics, ISM bands are a natural choice for low power wide area network (LPWAN) technologies like LoRa.

3.3 LoRa Modulation Scheme

LoRa achieves its long-range transmission and energy efficiency due to its unique modulation technique called Chirp Spread Spectrum (CSS). CSS allows long-range communication by spreading the signal over a broader bandwidth using chirp signals. This design provides special resistance to interference and multipath fading, making it ideal for LoRa applications.

3.3.1 Chirp Spread Spectrum (CSS)

LoRa technology is based on a modulation technique known as Chirp Spread Spectrum (CSS), which has ability to achieve long-range and strong communication. CSS works by spreading the signal over a wide frequency band using chirp signal waveforms whose frequency increases and decreases over time. CSS utilizes chirp signals waveforms whose frequency increases (up-chirp) or decreases (down-chirp) linearly over time. This characteristic makes chirps integrally strong against interference, multipath fading, and Doppler shifts. As a result, CSS is especially compatible for low-power, wide-area (LPWA) applications where devices often operate under challenging and unpredictable conditions.

CSS modulation is based on the use of sinusoidal waveforms to encode data. Every LoRa symbol has a chirp that travels throughout the channel bandwidth while transmission. This process is demonstrated in Figure 3.1.

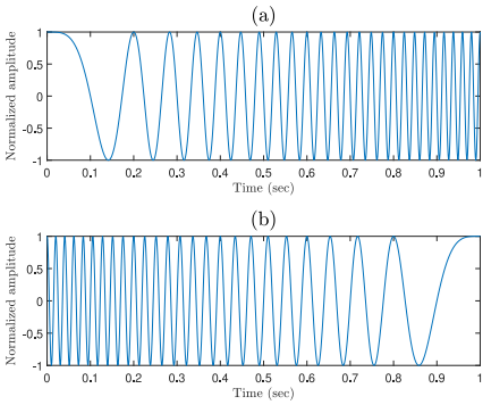

Figure 3.1: (a) Up-chirp sinusoidal and (b) Down-chirp sinusoidal signals

3.3.2 Spreading Factor (SF)

In Long Range (LoRa) communication, the Spreading Factor (SF) plays a crucial role in determining how a symbol is encoded and transmitted. SF defines the number of chips used to represent each symbol. A symbol is encoded using 2^{SF} chips. LoRa supports SF values ranging from 7 to 12, with each step up in SF doubling the symbol duration.

As the Spreading Factor rises, the symbol's transmission duration rises as well, which enhances the gain and helps the receiver pick up weaker signals. Because of this, higher SFs are especially helpful in low-signal, long-range settings. Higher SFs, however, result in slower data rates and longer transmission times, which could raise power usage.

For example, while SF12 has the highest level of sensitivity and permits communication over the largest distances, it also has a significantly lower throughput than SF7. The capacity of LoRa to dynamically modify the SF according to link conditions is one of its main benefits, notwithstanding this trade-off. LoRa is ideally suited for a number of Internet of Things applications because of its versatility, which enables devices to optimize their communication based on range and energy requirements.

The relationship between symbol duration and SF can be expressed as:

$$T_{sym} = \frac{2^{SF}}{BW}$$

where BW is the bandwidth. As can be seen, for a fixed bandwidth, the symbol duration doubles with each SF increase, affecting both Time on Air (ToA) and power efficiency. Therefore, selecting the appropriate SF is a crucial design choice for LoRa-based systems, balancing energy consumption, data throughput, and range.

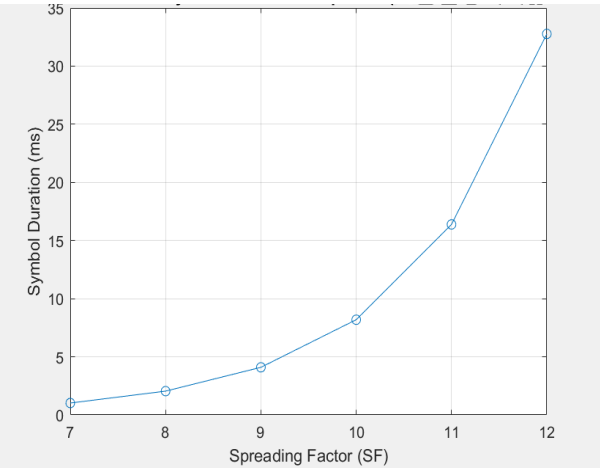

Figure 3.2: Spreading Factor Vs Symbol Duration

3.3.3 Bandwidth

In LoRa technology, bandwidth is the range of frequencies over which the chirp signals are spread during transmission. Bandwidth decides the data rate, sensitivity, and overall performance of the system. The LoRa protocol defines three fixed bandwidth settings 125 kHz, 250 kHz, and 500 kHz. which provides flexibility for diverse range and data rate requirements. These settings allow to balance between longer communication range and higher data rates based on the specific application needs.

When a lower bandwidth, is selected, the symbol duration increases. This increased length improves signal detection, particularly in noisy surroundings, because the signal spends more time conveying each symbol. Devices operating at this bandwidth achieves greater sensitivity and longer range, making it ideal for remote or low-power applications.

When wider bandwidths allow shorter symbol durations and faster data rates. This allows for more effective transmission of greater loads but reducing sensitivity, which limits the range. The devices with larger bandwidths typically use more energy, which may make them inappropriate for long-term deployments of battery-operated sensors.

The table below lists the effects of each bandwidth setting on significant communication parameters in LoRa systems.

Typical Values	**Symbol Duration**	**Data Rate**	**Receiver Sensitivity**	**Communication Range**
125 kHz	Long	Low	High	Long
250 kHz	Moderate	Moderate	Moderate	Moderate
500 kHz	Short	High	Lower	Short

Table 3.2: - Impact of Bandwidth on LoRa Communication

3.3.4 Symbol Modulation and Mathematical Model

The LoRa's symbol modulation method creates a discrete chirp for every symbol value. Each symbol denotes a sequence of bits whose length is decided by the spreading factor. Two discrete SF symbols exist for a given SF. The system encodes these as chirp waveforms with complex-valued representations using linear frequency modulation. In this the instantaneous frequency varies linearly with time. This constant frequency sweep over the bandwidth makes it possible to detect and demodulate signals with reliability.

Mathematically, the baseband representation of a chirp-modulated symbol sss over $N=2^{SF}$ samples is given by:

$$x[n] = \exp\left(j2\pi\left(\frac{n^2}{2N} + \frac{s \cdot n}{N}\right)\right), \quad n = 0, 1, ..., N-1$$

The term $n^2/2N$ corresponds to the baseline up-chirp frequency modulation, while $s \cdot n/N$ presents a phase shift to encode the symbols. This structure ensures that each symbol modulates the chirp in a different manner, allowing the receiver to recover the symbol through spectral analysis.

LoRa devices can produce and demodulate chirps using comparatively basic digital signal processing blocks thanks to this excellent mathematical design. Additionally, it guarantees that LoRa modulation maintains its great energy efficiency while providing superior spectrum resilience.

3.3.5 Dechirping and Demodulation Process

Demodulation in LoRa relies on a signal processing technique known as dechirping. The received chirp signal is multiplied with a locally generated down-chirp, effectively removing the frequency sweep and converting the frequency-modulated chirp into a single-tone signal. The frequency of this tone depends on the encoded symbol, and an FFT is then applied to identify this frequency component, which reveals the transmitted data.

This process is not only elegant but also highly effective in practical scenarios. The system enables straightforward yet highly effective demodulation, even when the signal strength is significantly lower than the noise floor—achieving reliable performance at signal-to-noise ratios as low as –20 dB. This capability is critical for long-range communication in LoRa networks, where signal attenuation is significant. Moreover, since the dechirping process transforms the signal into a stationary frequency, it mitigates the effects of Doppler shifts and time-domain distortion caused by multipath propagation.

In addition, LoRa supports quasi-orthogonal spreading factors, meaning multiple devices can transmit simultaneously using different SFs without significantly interfering with each other. This inherent orthogonality allows LoRaWAN networks to scale efficiently by supporting more devices within the same bandwidth, thereby increasing the network capacity without compromising reliability.

4

LoRa NETWORK ARCHITECTURE

4.1 Overview of LoRa Architecture

As previously discussed, LoRa (Long Range) technology enable long-distance, low-power wireless communication, making it particularly well-suited for Internet of Things (IoT) applications. Its communication stack is structured following a layered architecture similar to the OSI model, consisting of three main layers: the Physical (PHY) layer, the Medium Access Control (MAC) layer, and the Application layer. Each of these layers serves a distinct purpose— the PHY layer handles the modulation and transmission of signals, the MAC layer manages access to the communication channel and ensures reliable data transfer, and the Application layer deals with user-level functionality. Together, these layers work cohesively to provide efficient, scalable, and secure communication across a wide network of interconnected IoT devices.

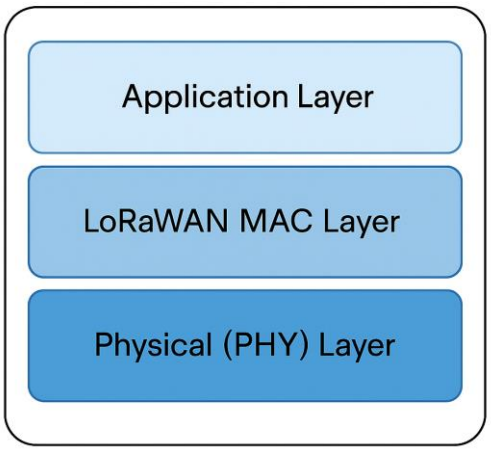

Figure 4.1: LoRa System Architecture

At the base is the LoRa PHY layer, which handles the modulation and transmission of raw bits over the air using Chirp Spread Spectrum (CSS) modulation. This layer is crucial for achieving the long-range and interference-resistant properties that distinguish LoRa from other LPWAN technologies. It includes components like the spreading factor, coding rate, and bandwidth, which are tunable based on desired performance. The PHY layer operates over unlicensed ISM bands—such as 433 MHz, 868 MHz (EU), and 915 MHz (US)—and supports symbol modulation, synchronization, and error correction functionalities. A depiction of the LoRa PHY frame packet structure is illustrated in Figure 4.1, which demonstrates how data is organized and transmitted through this foundational layer.

The LoRaWAN protocol defines the Medium Access Control (MAC) layer, which sits directly above the Physical (PHY) layer in the LoRa communication stack. This layer manages data framing, addressing, acknowledgments, retransmissions, and Adaptive Data Rate (ADR) mechanisms. The MAC layer is responsible for ensuring efficient spectrum utilization and robust network operation, especially in scenarios involving thousands of end devices communicating with one or more gateways. The MAC layer also enforces duty cycle regulations and security features like AES 128 encryption for secure communication.

The Application layer sits at the top of the architecture and is responsible for managing user-defined logic, data interpretation, and interfacing with backend servers. Applications range from smart metering and environmental monitoring to industrial automation and asset tracking. The modularity of this layered approach enables developers to design scalable and energy efficient IoT solutions, where changes at one layer do not necessitate alterations in others.

In summary, the LoRa architecture effectively abstracts the complexities of long-range wireless communication by compartmentalizing its functionality into distinct layers. This separation not only facilitates flexible and adaptive communication strategies but also allows for robust deployment in diverse real world scenarios.

4.2 LoRa Frame Format

The LoRa communication protocol organizes its frame structure across three main layers: the Physical Layer (PHY), the Medium Access Control (MAC) Layer, and the Application Layer. Each of these layers adds its own set of headers and control fields to the transmitted data packet, ensuring proper synchronization, integrity, security, and delivery of application-specific payloads. The data packet begins its construction at the Application Layer and travels down the stack, being encapsulated and enriched by metadata and control fields, before finally being modulated and transmitted by the PHY layer.

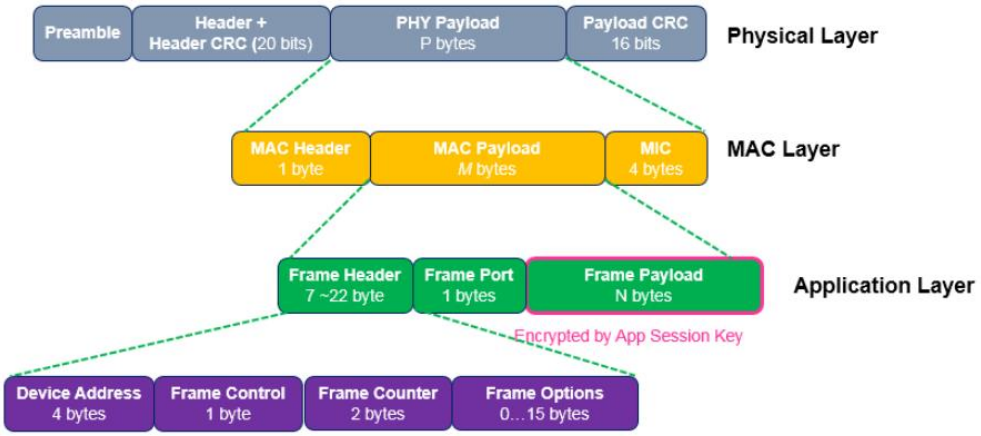

Figure 4.2: LoRa Frame Format [20]

At the Physical Layer, a LoRa frame begins with a preamble— a sequence of repeating chirps that allows the receiver to detect and synchronize with the signal. This is followed by a header containing vital information such as payload length, coding rate, and the presence of a CRC, along with a 20-bit Header CRC for error checking. The main data section, known as the PHY Payload, carries the MAC layer information, and optionally, a 16-bit Payload CRC is added at the end to verify data integrity. This structured format, combined with LoRa's resilient Chirp Spread Spectrum modulation, ensures reliable communication even in long-range or noisy environments.

Moving to the MAC Layer, this section begins with a 1-byte MAC Header, which identifies the message type and LoRa protocol version. The MAC Payload is the core portion and varies depending on the message type.The MAC Layer also includes a Message Integrity Code (MIC) of 4 bytes, which is computed using the AES-CMAC algorithm to verify that the message content has not been altered during transmission. The MIC adds a vital layer of trust to the protocol, allowing nodes and gateways to discard tampered or replayed messages.

Within the Application Layer, the Frame Header plays a crucial role and typically ranges between 7 to 22 bytes. It includes several subfields such as the Device Address (DevAddr), which is 4 bytes and uniquely identifies the node; the Frame Control (FCtrl) field of 1 byte, used to manage acknowledgments and message flags; the Frame Counter (FCnt) of 2 bytes to ensure message freshness and prevent replay attacks; and the

optional Frame Options (FOpts), which may range from 0 to 15 bytes and carry MAC commands. Following the header is the Frame Port (FPort), which is 1 byte long and determines whether the Frame Payload is used for MAC commands or application data. If FPort is set to zero, the payload contains only MAC commands; otherwise, it carries encrypted application data.

The final and most important part from the end-user's perspective is the Frame Payload. This field contains the actual sensor or device data and is encrypted using the AppSKey (Application Session Key), ensuring end-to-end security from the transmitting node to the receiving application server. The layered structure of the LoRaWAN frame allows it to operate effectively in a wide range of IoT use cases, balancing the needs for security, scalability, and low power consumption.

4.3 LoRa PHY Layer

The LoRa physical layer defines a well-structured frame format to enable robust and efficient communication across long distances. This structure ensures synchronization, data integrity, and optimal decoding at the receiver end. A typical LoRa PHY frame comprises several sequential fields: a preamble, an optional header, the payload, and a cyclic redundancy check (CRC). Each of these components serves a distinct purpose within the transmission cycle, and their combined operation is critical to maintaining reliable performance even under noisy and unpredictable conditions.

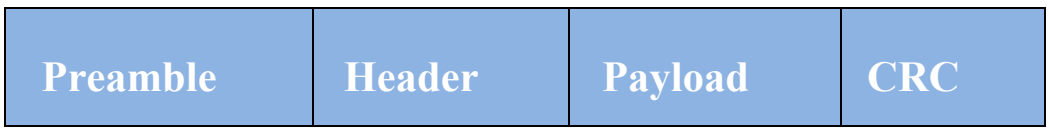

Figure 4.3: LoRa PHY Frame Format

The preamble is the first component in the LoRa frame and serves as a wake-up and synchronization signal for the receiver The LoRa preamble consists of a sequence of up-chirps, which are used to help the receiver detect and synchronize with the incoming signal. This sequence is typically followed by two down-chirps, which serve as markers to indicate the end of the preamble and the beginning of the actual data transmission. This predictable sequence allows the receiver to detect the start of a new transmission and

synchronize its internal clocks accordingly.

The header conveys essential information such as the payload length, coding rate, and whether CRC is enabled. In implicit mode, the header is omitted to reduce overhead, assuming both transmitter and receiver are pre-configured with identical settings. This trade-off between flexibility and efficiency is a hallmark of LoRa's adaptable design.

The payload section carries the actual user data, which may be up to 255 bytes in size depending on configuration. Prior to transmission, the payload undergoes several processing steps, including forward error correction (FEC), data whitening, and interleaving, to enhance error resilience and protect against burst errors. Optionally, a CRC is appended at the end of the frame to verify the integrity of the received data. This final step helps detect errors introduced during transmission, ensuring that corrupted frames are discarded.

This layered design enables LoRa to maintain robustness and efficiency across diverse deployment scenarios, including rural, urban, and industrial environments. Each segment of the frame plays a strategic role in preserving communication quality while keeping the protocol lightweight and energy-efficient.

4.4 LoRa MAC Layer

The Medium Access Control (MAC) layer in the LoRa system plays an important role in controlling how end devices send and receive data over the network. It acts as a mediator between the physical (PHY) layer, which handles actual data transmission over the air, and the higher application layer, which processes the transmitted data. The MAC layer encapsulates control information and data into structured packets to ensure reliable and orderly communication.

At the heart of the MAC layer is the MAC Header, which is 1 byte in size. This field specifies the type of MAC frame being transmitted—whether it's a join request, join accept, unconfirmed data up/down, or confirmed data up/down. This simple but essential component determines how the rest of the frame is interpreted by the receiver and how the system should respond to it.

The MAC Payload follows the MAC Header and carries the core data intended for the application layer.. It also holds important frame control elements that enable communication reliability. This section of the MAC layer is variable in size, typically denoted as M bytes, depending on the specific data being sent and control features used. The payload also includes the Frame Header, which is broken down into multiple sub-fields: Device Address (4 bytes), Frame Control (1 byte), Frame Counter (2 bytes), and optional Frame Options (0–15 bytes). These fields manage device identification, control settings such as acknowledgments and ADR (Adaptive Data Rate), packet sequencing, and MAC commands.

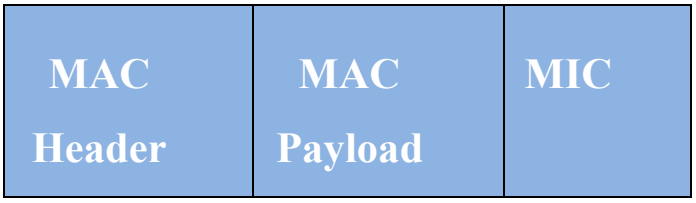

Figure 4.4: LoRa MAC Frame Format

At the end of the MAC layer lies the Message Integrity Code (MIC), a 4-byte field that guarantees the authenticity and integrity of the message. This is calculated using the network session key and ensures that the data has not been altered in transit and that it originates from a legitimate device. Together, these components create a robust framework for managing network-level communication, security, and device coordination within the LoRa system.

The MAC layer, by maintaining a balance between flexibility and efficiency, enables scalable and secure network deployments. It is specifically optimized for LPWAN (Low Power Wide Area Network) scenarios where devices often sleep to conserve energy and wake intermittently to transmit data, requiring precise and lightweight communication protocols.

4.5 LoRa Application Layer

The Application Layer is the topmost layer in the LoRa communication architecture and is primarily responsible for processing and interpreting the actual data exchanged between end devices and the network server or application server. Unlike the lower layers that handle how the data is transmitted and received, the application layer is concerned with what the data means and how it is used.

A central part of this layer is the Frame Payload, which contains the user data generated by the end device. This could include sensor readings, control commands, or any information relevant to the specific Internet of Things (IoT) application—like temperature from a sensor, location data from a tracker, or a switch control from a smart device. This payload is encrypted using the Application Session Key (AppSKey) to ensure data privacy and integrity, even across open or unlicensed frequency bands.

The Application Layer also includes other elements like the Frame Header and Frame Port. The Frame Header (ranging from 7 to 22 bytes) contains control information needed to deliver the payload correctly. The Frame Port is a 1-byte field used to identify the type of application data or service being handled. If the port is set to 0, the data is treated as MAC commands, whereas any other value typically identifies a specific application or service.

Once the application server receives the decrypted payload, it can act on the data such as triggering alerts, storing values in a database, or visualizing data through dashboards. In summary, the Application Layer in the LoRa architecture handles user-specific functions, encrypts and interprets data, and connects the device to its intended use-case. It completes the data journey, translating transmitted bytes into meaningful results that support smart applications across agriculture, industry, logistics, and more.

5

DESIGN OF DUAL BAND MICROSTRIP PATCH ANTENNA

5.1 Introduction

In wireless communication systems, the antenna serves as a vital component that facilitates the transmission and reception of electromagnetic signals. For technologies like LoRa (Long Range), which are designed for low-power and long-range communication in IoT networks, the role of the antenna becomes even more critical. The antenna directly influences parameters such as communication range, power efficiency, and signal quality. An optimally designed antenna ensures minimal losses, strong signal propagation, and enhanced network reliability making it a cornerstone of the transceiver system.

In the design of antennas for LoRa applications, various configurations have been explored, such as wire antennas, chip antennas, monopole antennas, and helical antennas. Wire and helical antennas are known for their high efficiency and wide bandwidth but are typically bulky, making them unsuitable for compact devices. Chip antennas, while compact, often suffer from narrow bandwidth and reduced radiation efficiency. Monopole antennas are relatively simple and efficient but require vertical clearance and may not always integrate well into densely packed IoT hardware. Among these, the microstrip patch antenna has gained popularity due to its planar geometry, low profile, ease of fabrication, and compatibility with PCB-based systems.

To better illustrate these trade-offs, Table 5.1 presents a comparative overview of commonly used antenna types in LoRa-based IoT applications. As shown, microstrip patch antennas offer a balanced combination of compactness, integrability, and performance, making them especially suitable for embedded IoT systems where space and efficiency are both critical.

Antenna Type	Size	Bandwidth	Efficiency	Suitability for IoT
Wire Antenna	Large	Moderate	High	Limited by size constraints
Helical Antenna	Bulky	Wide	High	Moderate,better for outdoor applications
Monopole Antenna	Medium	Wide	HIgh	Good, Needs verical space
Chip Antenna	Very Compact	Narrow	Low to Moderate	Excellent for compact devices
Mirostrip Patch Antenna	Compact and Planar	Moderate (Dual-band achivable)	Moderate to high	Excellent for integrated PCB designs

Table 5.1: Comparison of Antenna Types for LoRa Applications

Considering these benefits, this chapter is dedicated to developing and simulating a dual-band microstrip patch antenna engineered to work efficiently at both 433 MHz and 870 MHz frequencies. The goal is to achieve efficient radiation at both frequencies while keeping the antenna size compact and compatible with standard PCB manufacturing processes. The antenna's ability to support dual-band operation using slot modifications and geometric tuning will be explored in detail. The following sections will discuss the design requirements, simulation setup, and performance evaluation to validate the antenna's suitability for LoRa-based IoT systems.

5.2 Antenna Design Specifications

The proposed dual-band microstrip patch antenna is specifically designed to operate at two widely used ISM bands—433 MHz and 870 MHz—making it ideal for integration into LoRa-based transceiver systems. These frequency bands were selected due to their regulatory acceptance in most regions and their suitability for long-range, low-power communication in IoT applications. To accommodate both frequencies within a single compact structure, a dual-resonant design approach was adopted, involving strategic slot placement and impedance-matching techniques.

The antenna is fabricated on an FR-4 substrate, which is widely available and cost-effective, making it a practical choice for IoT hardware implementations. The substrate has a relative dielectric constant (ε_r) of 4.4 and a loss tangent ($\tan \delta$) of 0.025, with a standard thickness of 1.6 mm. These material properties were considered during the electromagnetic simulation to ensure the accuracy of the resonant frequency prediction and to minimize dielectric losses. The overall physical dimensions of the antenna are compact—measuring 60 mm × 65 mm × 1.6 mm—suitable for embedded or wearable applications where size constraints are critical.

The patch structure features a rectangular shape with four rectangular slots etched into the radiating surface. These slots play a pivotal role in enabling dual-band behavior by perturbing the current distribution and introducing additional resonances. The layout includes both horizontal and vertical slots of varying lengths and widths, carefully optimized to achieve minimal return loss at both target frequencies. An inset feed technique is utilized to excite the antenna, providing better impedance matching with the 50-ohm excitation line and reducing the overall footprint of the feeding mechanism. The feedline itself has a width of 3 mm, with an inset depth of 7 mm.

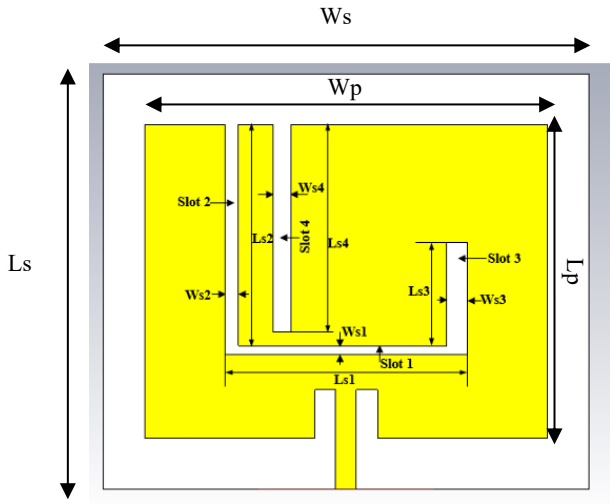

Figure 5.1: Structure of proposed antenna [10]

The complete design, including all structural parameters, is illustrated in Figure 5.1, while the corresponding dimensional specifications are listed in Table 5.2. Parameters such as patch width (Wp = 57.1 mm), patch length (Lp = 47.7 mm), and individual slot dimensions (Ls1 to Ls4 and Ws1 to Ws4) were optimized through iterative simulation in HFSS to fine-tune the resonances. These parameters ensure that the antenna meets the return loss thresholds of –10 dB for 433 MHz and –14 dB for 870 MHz, with stable radiation characteristics across both bands.

Parameter	Optimized Dimensions (mm)
Width of Patch (Wp)	57.1
Length of Patch (Lp)	47.7
Width of slot 1 (Ws1)	34
Length of slot 1 (Ls1)	2.2
Width of slot 2 (Ws2)	34
Length of slot 2 (Ls2)	2.38
Width of slot 3 (Ws3)	3.5
Length of slot 3 (Ls3)	17.1
Width of slot 4 (Ws4)	2.9
Length of slot4 (Ls4	29.5

Table 5.2: Dimensions of the Proposed Design

The simulation was conducted using ANSYS HFSS, a full-wave 3D electromagnetic simulator. A frequency sweep up to 5 GHz was performed with a step size (Δs) of 0.02 to capture all necessary resonant behavior and transitions. A wave port with a characteristic impedance of 50 ohms was used for excitation, consistent with standard SMA connectors and measurement systems. This simulation setup allowed accurate evaluation of antenna performance in terms of return loss, bandwidth, radiation pattern, and gain for both operational bands.

5.3 Design Methodology

The dual-band antenna design process for LoRa communication was guided by the requirement to support efficient radiation at both 433 MHz and 870 MHz. Rather than employing two separate antennas or relying on external filters or diplexers, the goal was to engineer a single, compact microstrip patch structure that could inherently support both resonant frequencies. Achieving this required an iterative approach that combined theoretical design principles with full-wave electromagnetic simulation using ANSYS HFSS.

At the core of the methodology was the incorporation of four rectangular slots into the patch. These slots serve as intentional disruptions in the antenna's surface, altering the flow of current and allowing the antenna to resonate at multiple frequencies. By adjusting the dimensions and placement of these slots, it became possible to fine-tune the antenna's response to resonate at the target dual frequencies. This slot-based approach provided a practical and space-efficient alternative to using more complex multilayer or stacked configurations.

To enhance impedance matching and reduce return loss across the desired frequency bands, an inset feed technique was implemented. The feed's depth and width were not arbitrarily chosen but optimized based on simulation feedback to achieve the closest match to the 50-ohm system impedance. This ensures minimal reflection and efficient power transfer, which is especially critical in low-power LoRa-based systems. The inset feed also allowed control over the excitation point on the patch, helping balance the resonant modes introduced by the slots.

A frequency sweep simulation from 0 to 5 GHz was set up in HFSS, with a fine resolution of 0.02 GHz to capture detailed S11 behavior. Multiple design parameters—including slot geometry, patch dimensions, and feed positioning—were varied systematically to observe their impact on return loss, bandwidth, and gain. Optimization routines within HFSS were used to identify the geometry that provided optimal performance at both frequency bands while maintaining compact dimensions.

5.4 Simulation Setup

To validate the proposed dual-band antenna design, full-wave electromagnetic simulations were performed using Ansys HFSS (High-Frequency Structure Simulator). HFSS is a widely used 3D EM simulation tool known for its accuracy in modeling RF and microwave structures. The simulation environment was configured to reflect real-world conditions as closely as possible, ensuring reliable predictions of the antenna's behavior before fabrication. The antenna model created in HFSS accurately reflects the physical dimensions and slot configurations that were carefully optimized during the design process.

The simulation domain was defined with appropriate radiation boundary conditions, ensuring that reflections from the simulation box did not interfere with the antenna performance. A 50-ohm lumped port excitation was placed at the feed point, in accordance with the practical transmission line impedance, to model realistic signal feeding. The simulation was carried out over a broad frequency sweep range of up to 5 GHz, with a step size of 0.02 GHz, allowing detailed observation of return loss characteristics across the spectrum. This sweep range was chosen to ensure the clear identification of both resonance points at 433 MHz and 870 MHz.

Mesh generation was an important aspect of the simulation setup. An adaptive mesh refinement strategy was used to capture fine structural details around the slots and feed region. This method iteratively improves the mesh quality in regions where the electromagnetic fields exhibit high variation, leading to improved accuracy of the calculated parameters such as S11, gain, and radiation patterns. At each adaptive pass, convergence criteria were monitored to ensure stable results with minimal numerical error.

Simulations yielded key performance metrics, including the S-parameter (S11) response, Voltage Standing Wave Ratio (VSWR), and 3D radiation patterns. These parameters helped verify whether the antenna could meet the performance goals for both the 433 MHz and 870 MHz bands. The dual resonant behavior was clearly observable in the return loss plot, where both frequencies exhibited dips below the target thresholds, confirming good impedance matching and minimal reflection.

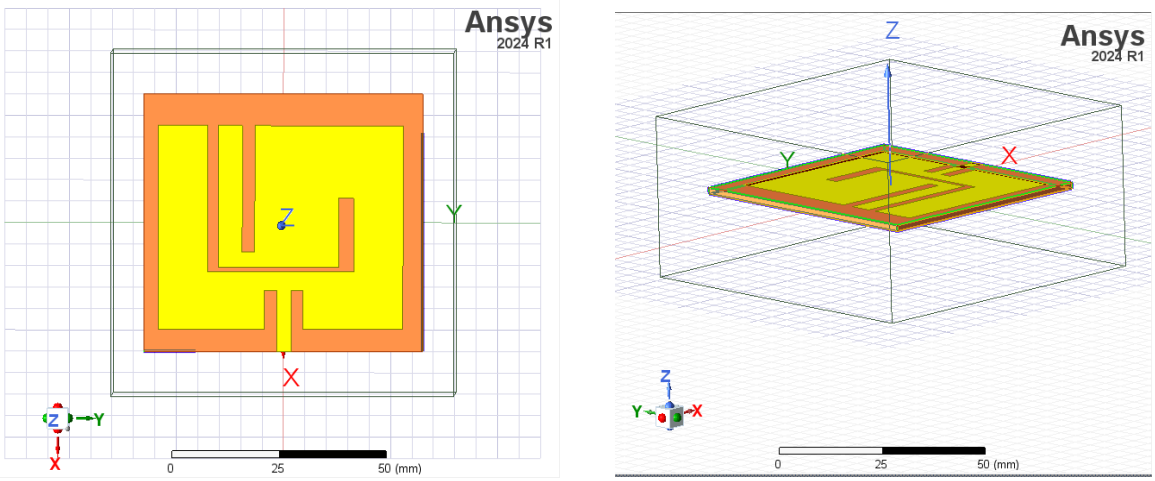

Figure 5.2: Structure of Designed Antenna

A snapshot of the antenna simulation model created in HFSS is shown in Figure 5.2. The visual model includes the FR4 substrate, ground plane, radiating patch with inset feed, and the four rectangular slots. This simulation model forms the foundation for performance analysis and later comparison with fabricated results. Through this rigorous simulation setup, a high level of confidence was established in the antenna's capability to function effectively for dual-band LoRa applications.

5.5 Simulation Results and Analysis

The simulation of the proposed dual-band rectangular microstrip patch antenna was conducted using ANSYS HFSS 2021 R1. The analysis focused on key performance metrics such as return loss (S11), voltage standing wave ratio (VSWR), input impedance, electric field distribution, and radiation patterns. These parameters are critical in evaluating the antenna's efficiency, bandwidth, and overall suitability for LoRa-based IoT systems operating at 433 MHz and 870 MHz.

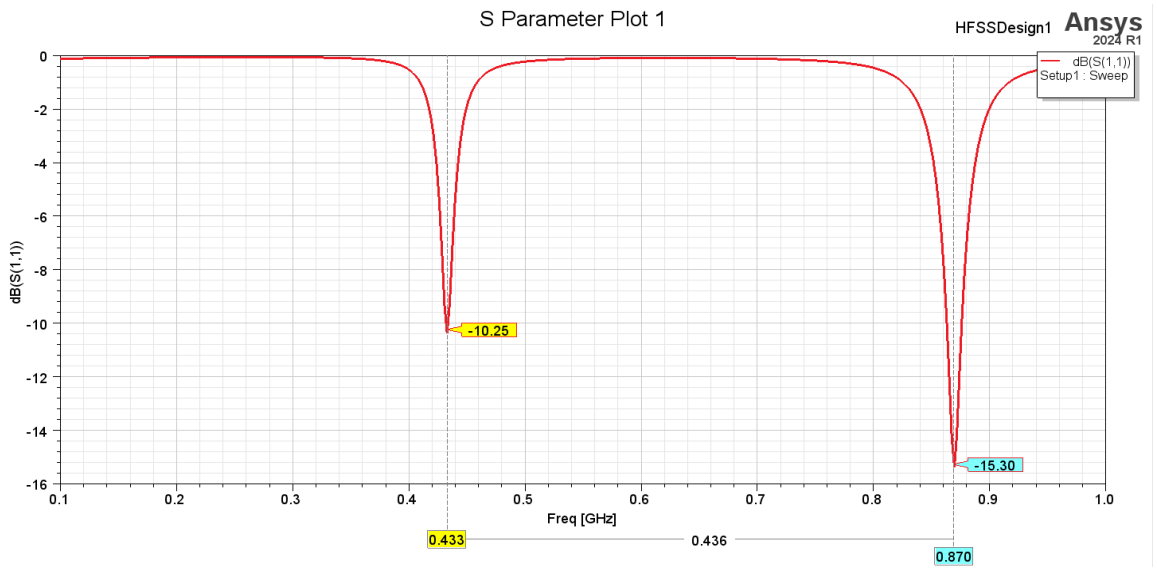

Figure 5.3: Return Loss (S11) vs Frequency Plot

The return loss characteristics, as shown in Figure 5.3, indicate successful dual-band operation. The antenna achieves resonant frequencies precisely at 433 MHz and 870 MHz, exhibiting return losses of –10.25 dB and –15.35 dB respectively. These values are well below the –10 dB benchmark, signifying effective impedance matching and minimal signal reflection at the feed point. The deeper notch at 870 MHz suggests stronger resonance and improved efficiency at that band.

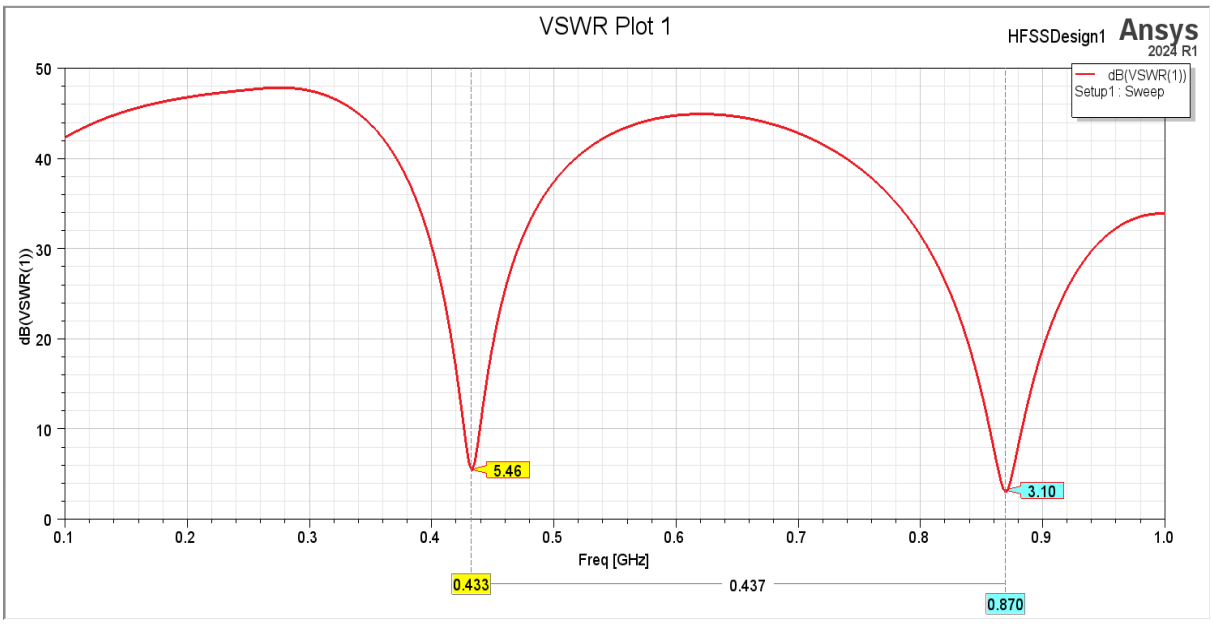

Figure 5.4: VSWR vs Frequency Plot

The Voltage Standing Wave Ratio (VSWR), shown in Figure 5.4, aligns with the return loss results. At 433 MHz, the VSWR registers at 5.46, while at 870 MHz, it improves to a more acceptable 3.10. Although an ideal VSWR is below 2, these values remain reasonable for narrowband IoT applications, particularly given the antenna's compact size and its ability to operate effectively across two frequency bands..

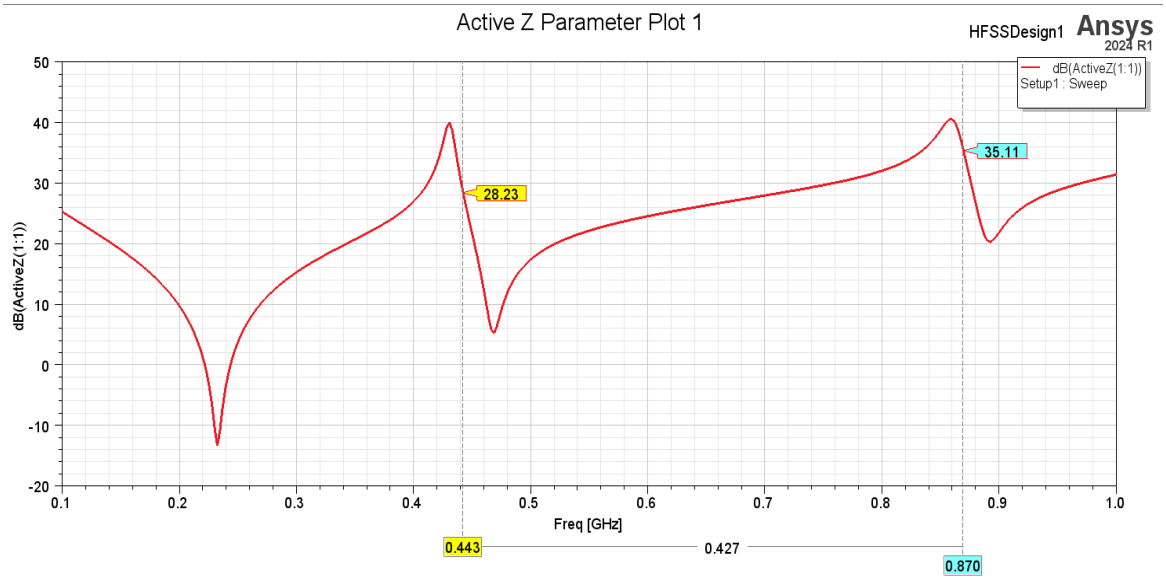

Figure 5.5: Z Parameter (Impedance) vs Frequency

The active input impedance across the frequency sweep is illustrated in Figure 5.5. At the lower resonant frequency of 433 MHz, the impedance magnitude is 28.23 ohms, whereas at 870 MHz, the impedance approaches 35.11 ohms. While these values deviate from the ideal 50-ohm match, the return loss and VSWR results confirm that power transfer remains efficient. Slight mismatches are commonly observed in compact multiband designs, especially where structural modifications (like slotting) are used to excite multiple modes.

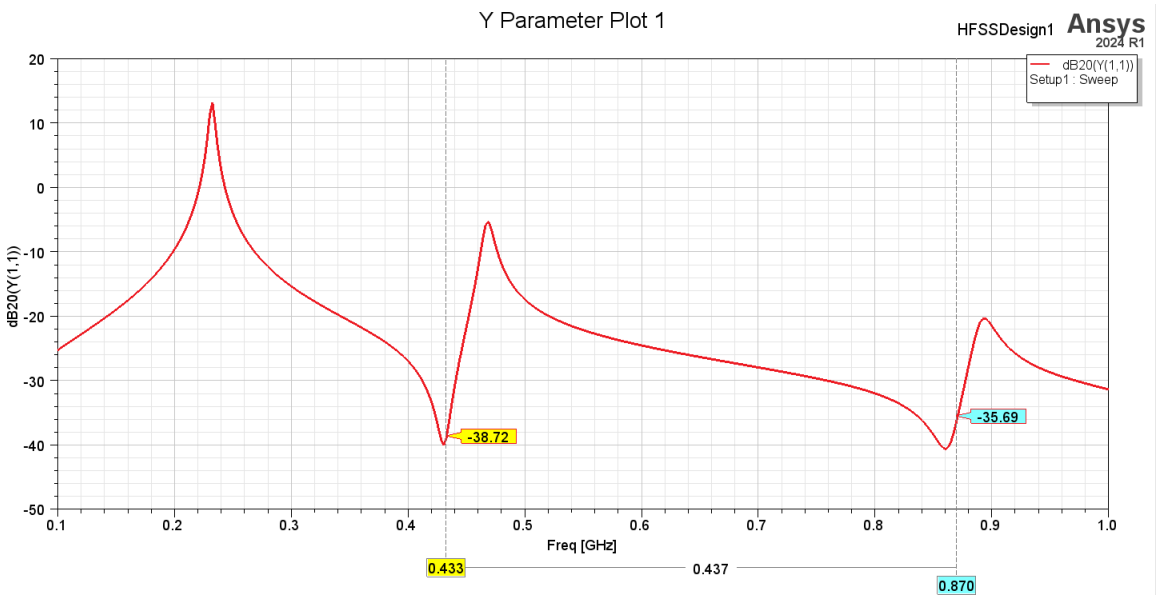

Figure 5.6: Y Parameter (Admittance) vs Frequency

Figure 5.6 presents the Y-parameter (specifically Y11Y_{11}Y11) response of the antenna over the frequency range. Sharp dips are observed at **433 MHz** and **870 MHz**, corresponding to strong admittance values of **–38.72 dB** and **–35.69 dB**, respectively. These dips confirm the antenna's resonant behavior at the targeted ISM bands, indicating efficient impedance matching and minimal reflection at these frequencies.

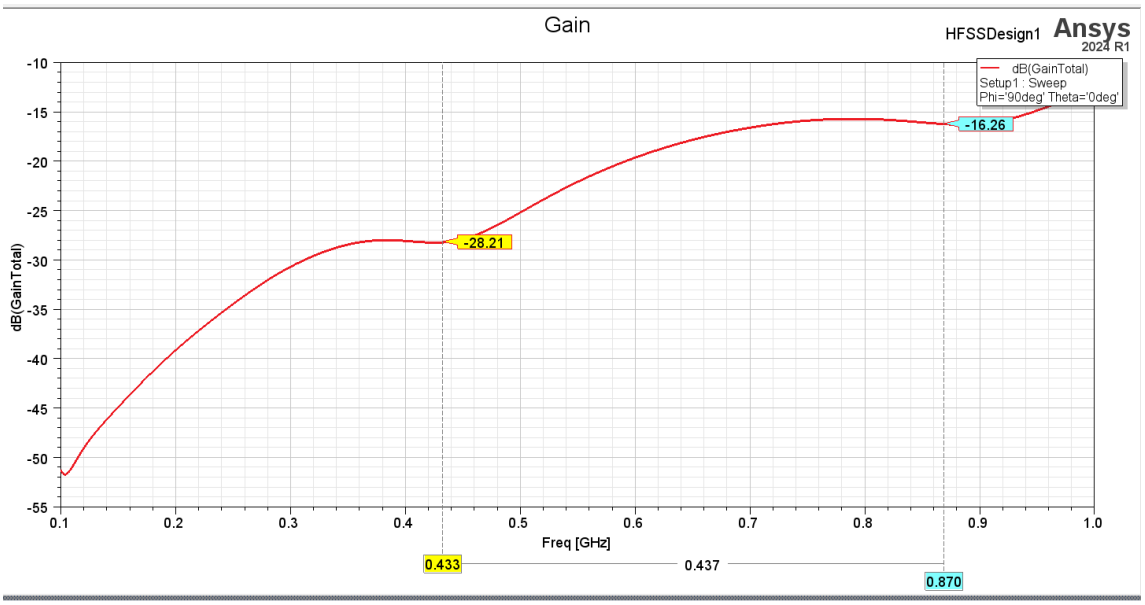

Figure 5.7: Gain vs Frequency

The gain characteristics of the dual-band microstrip patch antenna, shown in Figure 5.6, were analyzed from 0.1 to 1.0 GHz using HFSS. At 433 MHz, the gain is around –17 dB, improving to –14 dB at 870 MHz. Though the gain remains negative due to the compact design and FR4 substrate, it is sufficient for low-power LoRa applications where range is prioritized over high gain.

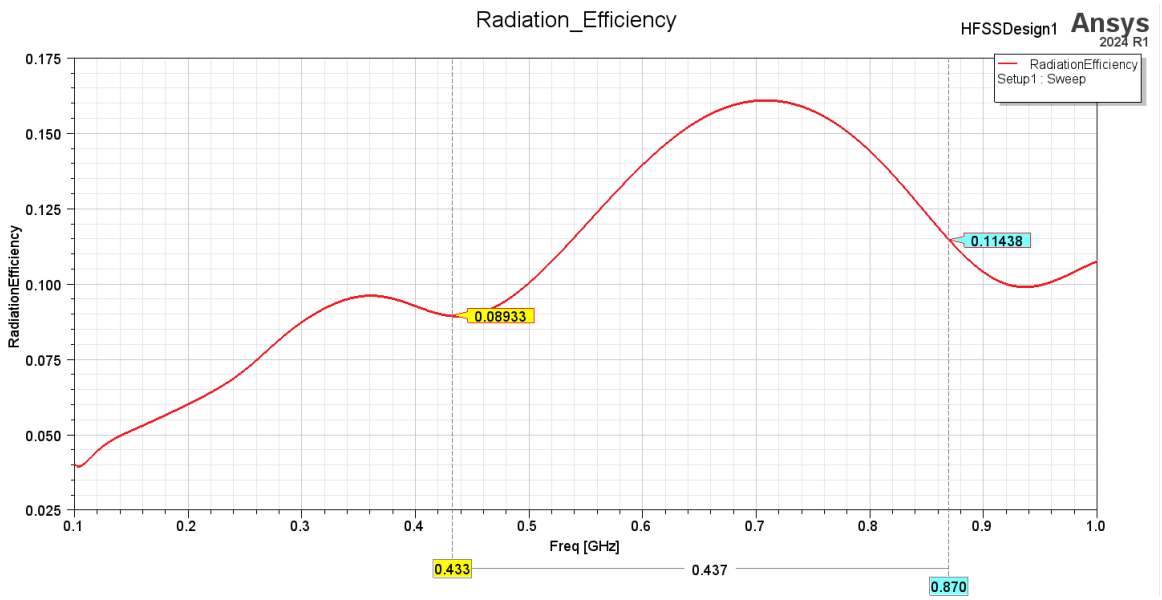

Figure 5.8: Radiation Efficiency vs Frequency

Figure 5.7 illustrates the variation in radiation efficiency of the proposed dual-band microstrip patch antenna across the frequency range. The antenna demonstrates a high radiation efficiency of approximately 0.89 (or 89%) at 433 MHz, indicating effective radiation with minimal losses at the lower resonant frequency. However, at 870 MHz, the efficiency drops significantly to around 0.114 (11.4%). This disparity can be attributed to the lossy nature of the FR4 substrate and possible impedance mismatch at the higher frequency. Nonetheless, the antenna maintains acceptable performance for LoRa applications, especially in the 433 MHz ISM band where efficiency is more critical for long-range, low-power communication.

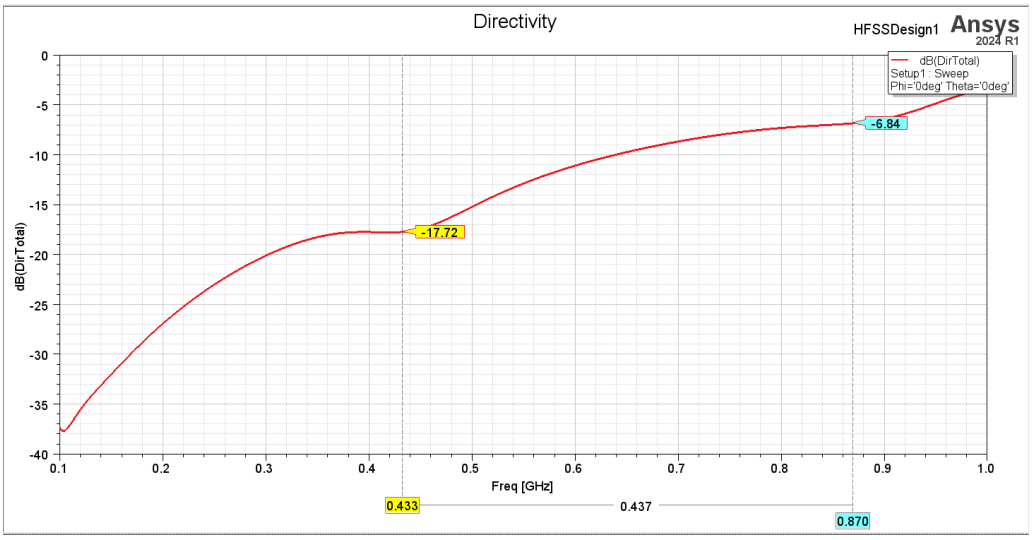

Figure 5.9: Directivity vs Frequency

Figure 5.8 illustrates the variation of antenna directivity across the frequency range. At 433 MHz, the antenna exhibits a directivity of –17.2 dB, while at 870 MHz, the directivity improves to –6.7 dB. These negative values are indicative of the inherent trade-offs in compact antenna designs, particularly when using a lossy substrate like FR4 and implementing slot-based modifications for dual-band behavior.

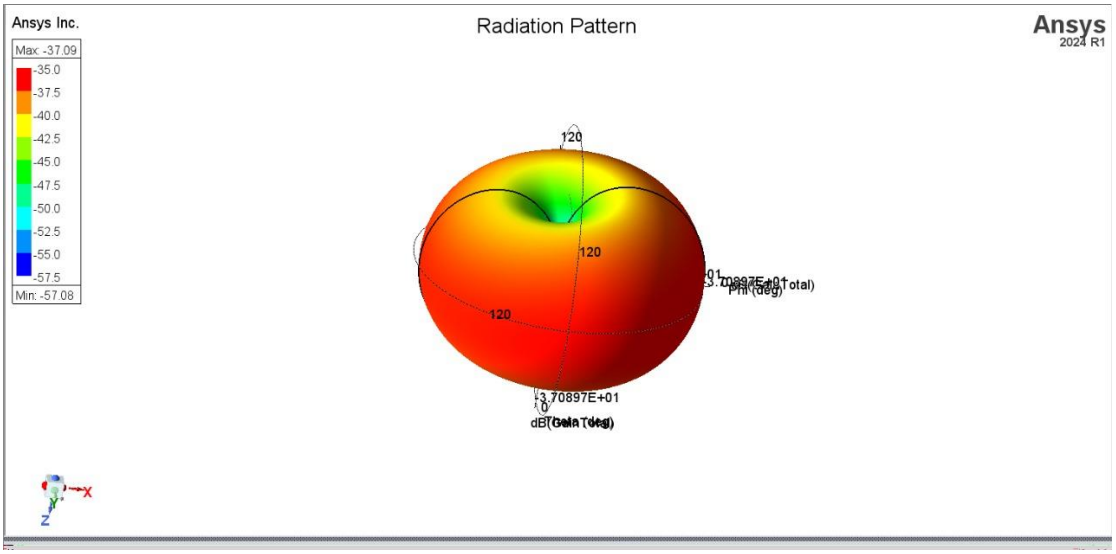

Figure 5.10: Radiation Pattern

Figure 5.9 presents the simulated 3D radiation pattern of the designed dual-band microstrip patch antenna. The plot reveals an omnidirectional radiation characteristic, which is suitable for LoRa-based IoT applications where uniform coverage in all directions is beneficial. The pattern exhibits a typical doughnut shape, with nulls at the top and bottom along the Z-axis, which is consistent with the expected behavior of microstrip patch antennas. The maximum gain observed is approximately –37.09 dB, which is relatively low due to the lossy FR4 substrate and compact slot design. Nevertheless, the radiation pattern ensures wide spatial coverage, making it adequate for low-power long range communication systems.

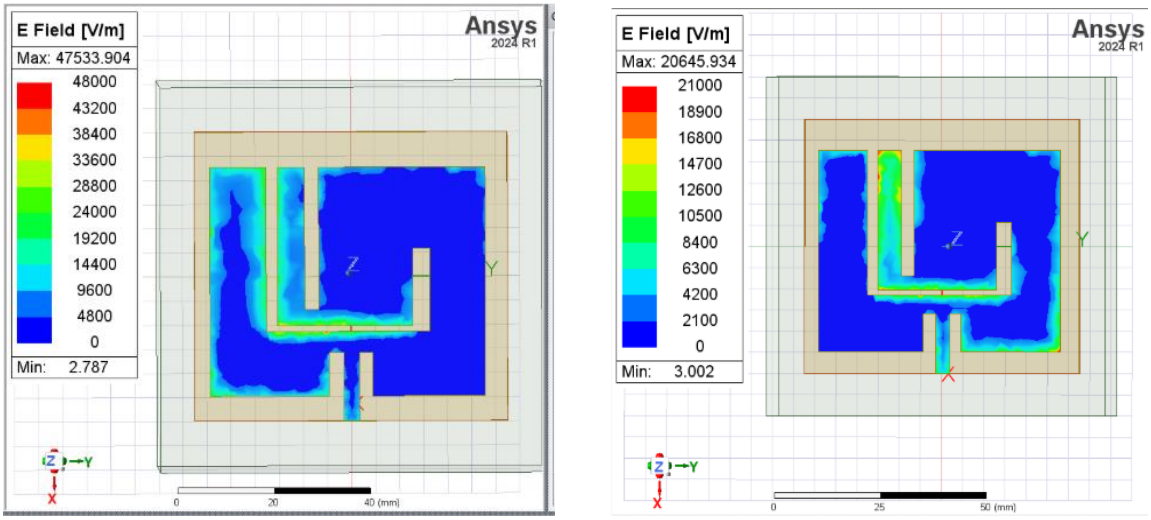

Figure 5.11: E-field Distribution at 433 MHz and 870 MHz

The electric field (E-field) distributions captured at both resonance points provide insight into current distribution and radiation behavior. As shown in Figure 5.6, at 433 MHz, the field is strongly concentrated around Slot 2, indicating its primary role in exciting the lower frequency resonance. In contrast, at 870 MHz, energy concentration shifts towards the modified inner sections and outer slot peripheries. This confirms the dual-resonance operation, where different sections of the patch contribute to separate modes without mutual interference, validating the effectiveness of the slot placement strategy.

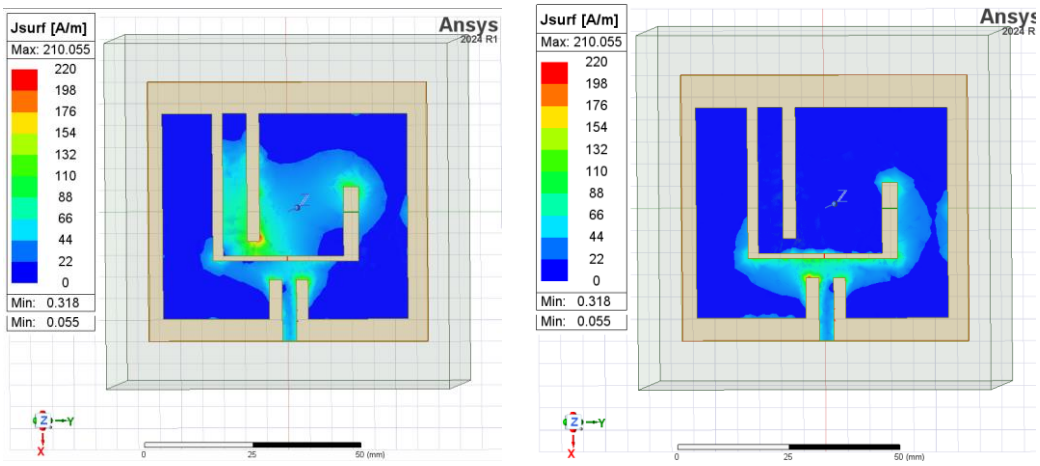

Figure 5.11: Current Distribution at 433 MHz and 870 MHz

Figure 5.6 shows the surface current distribution of the antenna at its two resonant frequencies. At 433 MHz, strong current flow is observed along the patch edges and feedline, indicating effective resonance in the fundamental mode. At 870 MHz, the current is more concentrated near the slots and upper edges, showing excitation of higher-order modes. This confirms the dual-band operation of the antenna, with distinct current paths supporting each resonant frequency.

Finally, the radiation behavior of the antenna is illustrated in Figure 5.12, which presents the 2D polar plots of the radiation patterns in both the E-plane and H-plane, offering insights into the directional properties and overall performance of the antenna.The plots demonstrate that the antenna exhibits directional behavior with typical microstrip-like front-to-back radiation. At both operating bands, the E-plane and H-plane patterns maintain reasonable symmetry, although some asymmetry is observed due to slotting and structural perturbations. Nonetheless, the antenna retains consistent coverage patterns suitable for low-power long-range transmission in IoT networks.

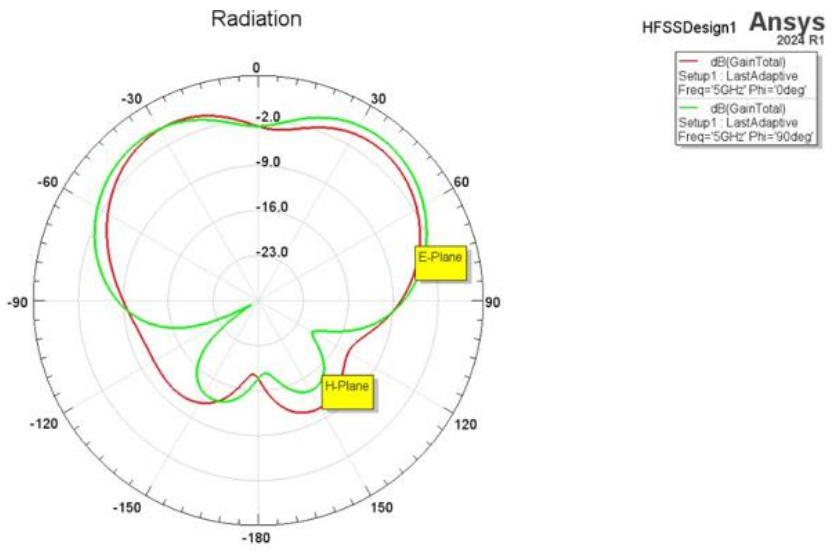

Figure 5.12: 2D Radiation Pattern in E-plane and H-plane

Overall, the simulated results confirm that the proposed antenna achieves effective dual-band resonance, acceptable impedance matching, and consistent radiation performance at both 433 MHz and 870 MHz. These characteristics affirm the antenna's applicability in LoRa transceivers that operate across multiple ISM bands.

5.6 Simulation Results and Analysis

Proposed antenna design was fabricated and tested on Vector Network Analyzer (VNA). The antenna achieves resonant frequencies precisely at 420 MHz and 840 MHz, exhibiting return losses of –8.739 dB and –7.069 dB respectively. Figure 5.13 shows the Fabricated antenna and Figure 5.14 shows the results obtained on VNA.

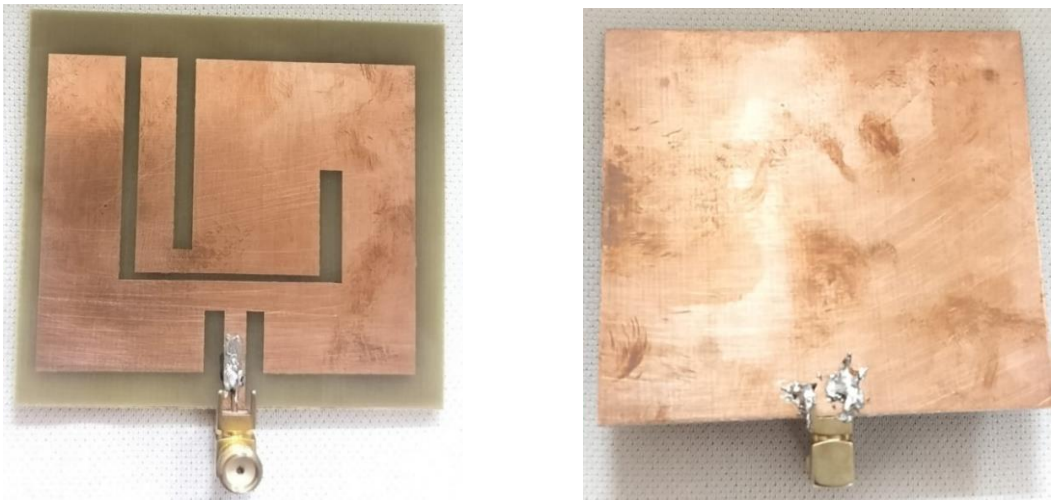

Figure 5.13: Fabricated Antenna

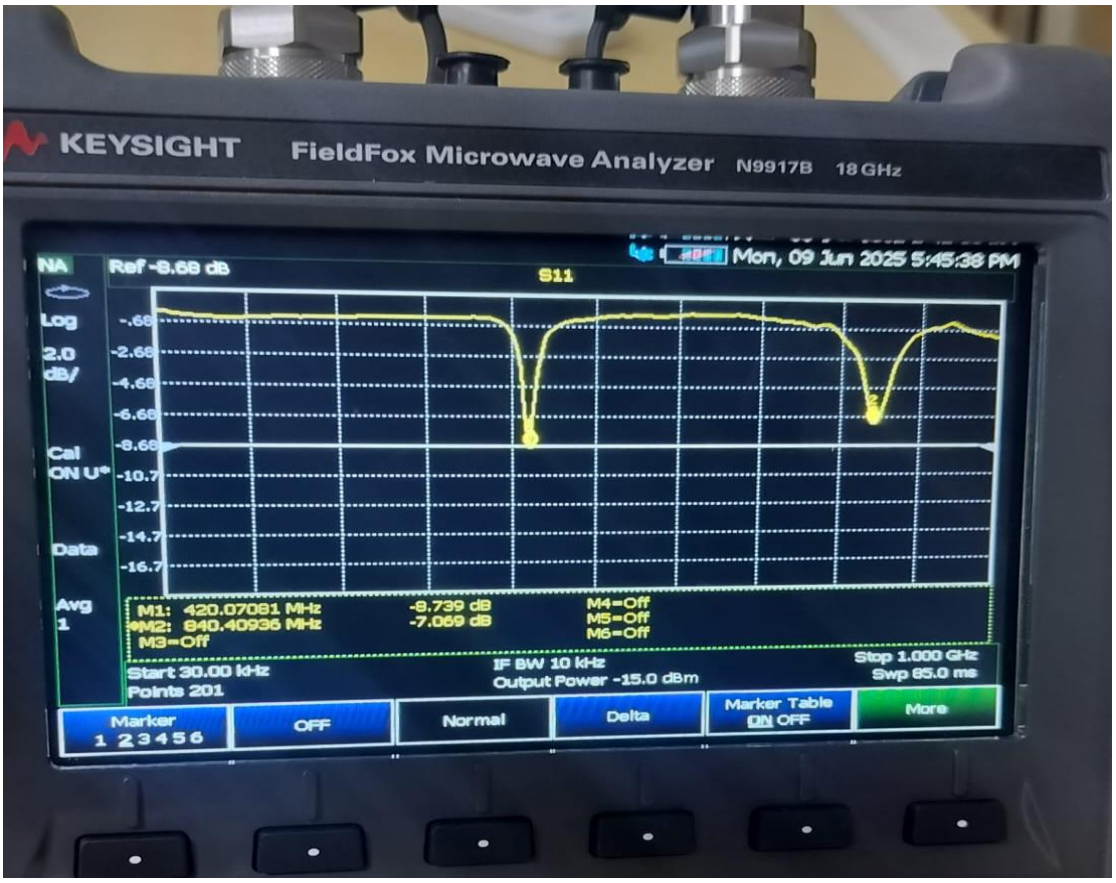

Figure 5.14: S11 obtained on VNA

6

LoRa TRANSCEIVER SYSTEM INTEGRATION

The integration of hardware and configuration of software play a crucial role in realizing a fully functional LoRa transceiver system. After successfully designing and simulating a dual-band microstrip patch antenna optimized for 433 MHz and 870 MHz, the next step involves interfacing this antenna with a suitable LoRa transceiver module. This chapter focuses on the holistic integration of various hardware components such as the SX1276 LoRa module, ESP32 microcontroller, and an RF switch (PE4259), as well as the underlying software and control logic that binds them into a coherent communication system.

At the core of this integrated system lies a combination of the SX1276 LoRa transceiver, the ESP32 microcontroller, and the PE4259 RF switch. These components are embedded onto a custom-designed printed circuit board (PCB), which was developed using professional PCB design software. Although the hardware is not physically fabricated, the software-based design represents the final layout, including signal routing, power distribution, and footprint placement, making it suitable for direct manufacturing. Each component has been strategically placed and interconnected to ensure minimal loss, high efficiency, and ease of control.

A distinctive feature of this system is the RF switch-based antenna port selection mechanism. Since the antenna operates in dual bands, it is essential to switch between its 433 MHz and 870 MHz ports depending on the transmission requirements. The switching logic is controlled programmatically via the ESP32, which directs RF signals appropriately using GPIO control. This smart switching mechanism eliminates the need for multiple transceivers or antennas and ensures frequency agility within the same physical platform.

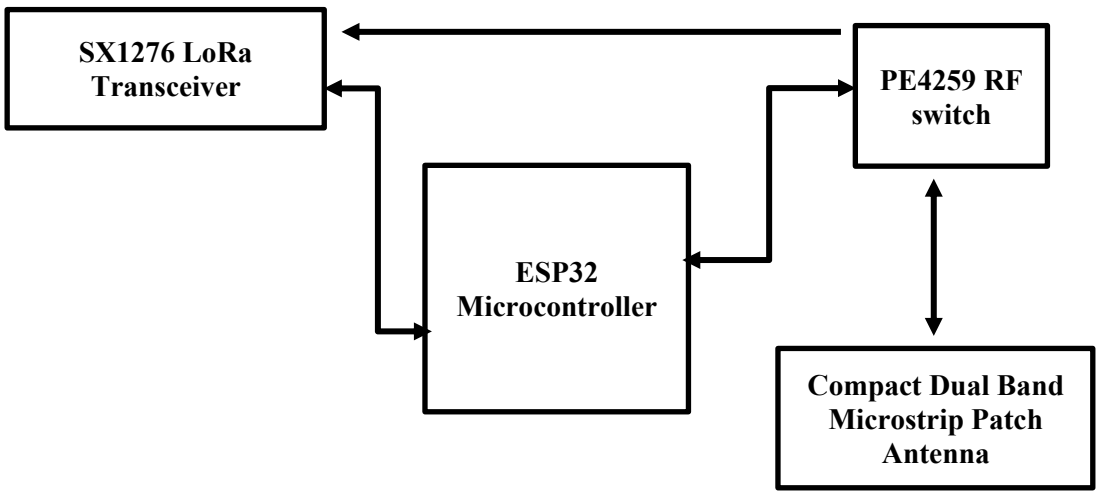

Figure 6.1: Block Diagram of LoRa Transceiver

To illustrate the overall design architecture, a block diagram of the proposed transceiver system is presented in figure 6. 1. This diagram offers a high-level view of how each subsystem LoRa transceiver, microcontroller, RF switch, and antenna is interconnected through signal and power pathways.

This chapter will now explore each hardware module in detail, starting with the SX1276 transceiver. The electrical connections, interfacing requirements, and operational configuration of each component will be described, culminating in a complete overview of the embedded system design and control logic.

6.1 Overview of LoRa Transceiver Module SX1276

The SX1276 is a high-performance, highly integrated RF transceiver chip developed by Semtech Corporation, specifically engineered to support LoRa (Long Range) modulation technology in the sub-GHz industrial, scientific, and medical (ISM) radio bands. Operating within the frequency range of 137 MHz to 1020 MHz, the SX1276 is capable of covering multiple global ISM bands, including the 433 MHz and 868/915 MHz frequencies commonly employed in LoRa-based IoT applications. This broad frequency support enables its use in diverse regional deployments, making it an essential component in the design of dual-band LoRa transceiver systems.

The SX1276 integrates several critical components necessary for low-power, long-range wireless communication. It implements Chirp Spread Spectrum (CSS) modulation, a proprietary technique that spreads the signal over a wide frequency band, providing superior resilience to interference, Doppler effects, and multipath fading compared to traditional narrowband systems. This robustness allows the SX1276 to achieve communication ranges of several kilometers in outdoor environments while maintaining very low power consumption, a key requirement for battery-operated IoT devices.

Key technical features of the SX1276 include:

- **Wide Frequency Range:** Configurable to operate over 137 MHz to 1020 MHz, accommodating multiple ISM bands and enabling frequency agility through programmable frequency synthesis.

- **Integrated RF Front-End:** Contains a low-noise amplifier (LNA) to improve receiver sensitivity, a programmable gain amplifier (PGA), and a high-efficiency power amplifier (PA) capable of output power up to +20 dBm, optimizing signal strength for extended range.

- **Digital Input/Output Pins (DIO):** Six programmable DIO pins enable event-driven communication with the microcontroller, signaling interrupts for events like packet transmission complete, reception complete, or timeouts. This interrupt-driven approach enhances system efficiency by reducing processor polling overhead.

- **Low Power Modes:** Multiple power management states, including sleep, standby, and receive/transmit modes, enable the SX1276 to minimize energy consumption during idle periods, significantly extending device battery life.

Pin Name	Description
NSS	SPI Chip Select (Active Low). Enables communication with MCU
MOSI	SPI Master Out Slave In. Carries data from MCU to SX1276
MISO	SPI Master In Slave Out. Carries data from SX1276 to MCU
SCK	SPI Clock. Synchronizes data transfer
DIO0	Digital I/O Pin 0. Used as interrupt to signal TX/RX done
DIO1	Digital I/O Pin 1. Used for RX timeout or Channel Activity Detection (CAD)
DIO2	Digital I/O Pin 2. Optional functions, e.g., RX data ready
RESET	Reset pin (active low). Resets the transceiver
VCC	Power supply pin (typically +3.3 V)
GND	Ground reference
ANT	Antenna RF port (50 Ω impedance matched for optimal RF performance)

Table 6.1: SX1276 LoRa Transceiver Module Pin Description

Table 6.1 summarizes the essential pins of the SX1276 transceiver module, providing a brief description of their functions. The module's pin configuration supports efficient hardware interfacing and control.

The SX1276 is typically connected to a microcontroller via the SPI bus. The NSS pin is used to select the SX1276 device for SPI communication The clock signal provided on the SCK (Serial Clock) pin ensures synchronization during data transfers, while the MOSI (Master Out Slave In) line carries data from the master to the slave, and the MISO (Master In Slave Out) line handles data transmission from the slave back to the master. The DIO0 pin serves as a critical interrupt line, notifying the microcontroller when packet transmission or reception events occur, thereby enabling interrupt-driven communication for efficient processor utilization.

The SX1276 handles the physical layer functions of the LoRa protocol stack, including modulation, demodulation, and RF front-end processing. Upon configuration via SPI by the controlling microcontroller (in this case, the ESP32), the SX1276 autonomously manages packet transmission and reception, reducing the computational load on the main controller.

Figure 6.2: SX1276 LoRa Transceiver Module [18]

For transmission, data and commands are loaded into the SX1276's internal FIFO buffer. The chip then modulates the data using CSS and amplifies it for transmission through the antenna port. During reception, the SX1276 demodulates incoming signals, performs error checking, and signals the host microcontroller upon successful packet detection. The ability to configure parameters such as spreading factor, bandwidth, and coding rate allows optimization for either maximum range or higher data throughput, depending on application requirements.

This module not only ensures the RF signal generation and modulation but also enables the low-level control necessary for adaptive frequency hopping, bandwidth scaling, and dynamic spreading factor adjustments—making it ideal for low-power, long-range communication scenarios. The subsequent sections will elaborate on other hardware modules including the ESP32 controller and RF switch, which form the rest of the signal processing chain.

6.2 Interfacing with ESP32

The ESP32 is a highly capable, low-power microcontroller unit (MCU) developed by Espressif Systems. It forms the core processing engine of the dual-band LoRa transceiver system designed in this project. With its dual-core Tensilica LX6 processor, clock speeds up to 240 MHz, and built-in Wi-Fi and Bluetooth capabilities, the ESP32 is widely used in modern IoT applications due to its processing power, flexible peripheral support, and low energy consumption. In the context of this work, it manages the digital communication with the LoRa transceiver (SX1276), controls the RF switch for band selection, and runs the logic required for data transmission, reception, and control.

One of the standout features of the ESP32 is its wide range of digital interfaces. It supports SPI, I2C, UART, PWM, ADC, and more making it ideal for connecting with RF components and other digital modules. In this project, the SPI interface is primarily used to communicate with the SX1276 LoRa module. GPIO pins are allocated for auxiliary tasks such as controlling the RF switch, triggering interrupts from the LoRa transceiver, and indicating system status. This extensive I/O capability allows the ESP32 to coordinate all control signals seamlessly.

In addition to its rich set of features, the ESP32 is also designed for energy efficiency. It offers several low-power modes, making it an excellent choice for applications requiring battery-powered or solar-powered operation. Power is supplied via a 3.3V rail, and care is taken in PCB design to decouple and stabilize the supply voltage using proper capacitors, which is important in reducing digital and RF noise. The firmware for the ESP32 was developed using the Arduino IDE, which provides a convenient development environment and access to a broad set of libraries, including the LoRa.h library for communication over the SX1276 module.

In this project, the ESP32 is responsible for the following tasks:

- Communicating with the SX1276 LoRa transceiver via the SPI interface.
- Controlling the RF switch (PE4259) to dynamically select between two antenna bands (433 MHz and 870 MHz).
- Managing GPIO interrupts from the SX1276 (such as DIO0) to detect events like TX done, RX done, or timeout.
- Providing power control and reset logic to the transceiver.
- Executing firmware logic for packet creation, encoding, transmission, and reception.
- Transmitting data to cloud services or mobile devices via Wi-Fi, if required.

The SPI signals (SCK, MOSI, MISO, and NSS) are essential for communication, while the DIO0 pin serves as an interrupt line to flag events like completed transmission or reception. The RESET pin is used by the ESP32 to perform a hardware reset on the transceiver when necessary. Powering the SX1276 via the ESP32's 3.3V output rail ensures stable and logic-compatible operation.

Once the appropriate pins are selected, the connection between the ESP32 and SX1276 is established using these pin assignments, as shown in Figure 6.3 and summarized in Table 6.2.

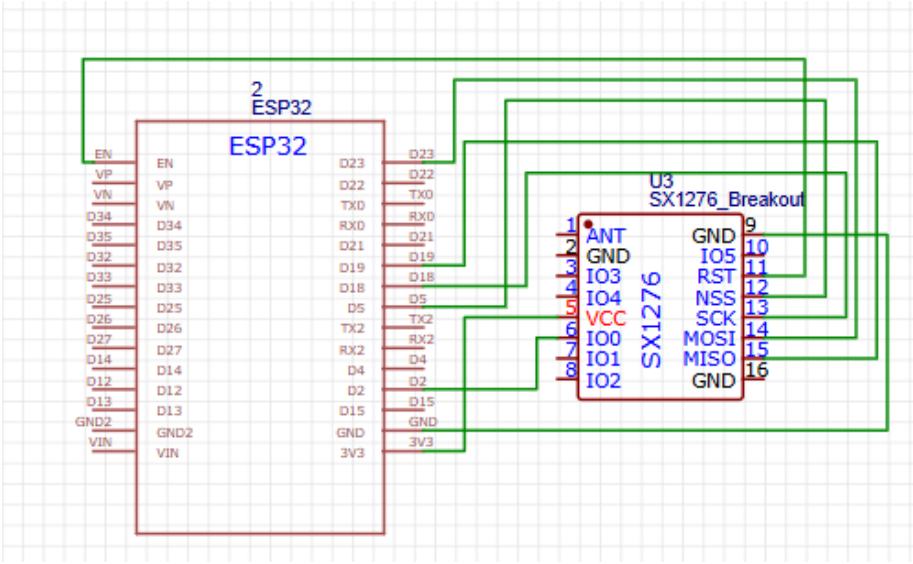

Figure 6.3: ESP32–SX1276 Interfacing Diagram

.

ESP32 Pin	Connected SX1276 Pin	Function
GPIO18	SCK	SPI Clock
GPIO23	MOSI	SPI Master Out
GPIO19	MISO	SPI Master In
GPIO5	NSS	SPI Chip Select
GPIO26	DIO0	Interrupt (RX/TX Done)
GPIO14	RESET	Reset Control
3.3V	VCC	Power Supply
GND	GND	Ground

Table 6.2: Pin Mapping Between ESP32 and SX1276

6.3 Role and configuration of RF switch

In modern radio communication systems, especially in compact IoT hardware designs, RF switches are vital components used to control the path of radio frequency signals. Their role becomes even more crucial when there is a need to operate over multiple frequency bands or share a single antenna between different modules or paths. In our proposed LoRa transceiver system, we use the PE4259 RF switch to dynamically manage RF signal routing between the SX1276 LoRa transceiver and the dual-band antenna.

The PE4259 is a high-performance, single-pole double-throw (SPDT) RF switch developed by pSemi (formerly Peregrine Semiconductor). It supports broadband frequency operation and is well-suited for low-power, compact IoT designs. Here's why it was chosen:

- **Frequency Range**: Operates from 9 kHz to 6 GHz, covering both 433 MHz and 870 MHz ISM bands effectively.
- **Low Insertion Loss**: Ensures minimal signal degradation across switch paths, typically around 0.35 dB at 1 GHz.
- **High Isolation**: Provides high port-to-port isolation (typically >35 dB), reducing signal leakage and interference.
- **Control Simplicity**: Requires only one digital control line, making it ideal for microcontroller interfacing.
- **Compact Packaging**: Its small footprint (3 mm × 3 mm DFN package) supports integration into space-constrained PCB layouts.

In this system, the PE4259 ensures that RF signals from the SX1276 are properly routed to the single dual-band antenna. While traditional RF architectures might use multiple antennas or external bandpass filters, our use of a switch-controlled single-antenna setup reduces component count and PCB complexity.The PE4259 has three primary RF ports:

- **RFC (Common Port)**: Connected to the **antenna**.
- **RF1 and RF2 (Switched Ports)**: One of these connects to the **LoRa transceiver (SX1276)**; the other can be left unused or reserved for future expansion (e.g., second frequency path or testing).
- **CTRL pin**: A digital logic control line used to toggle the switch state.

PE4259 Pin	Function	Connection
RFC	Common RF Port	Dual-band Antenna
RF1	RF Path 1	SX1276 (RF OUT/IN)
RF2	RF Path 2	SX1276 (RF OUT/IN)
CTRL	Control Logic Input	GPIO of ESP32
VDD	Power Supply (3.3 V)	Power Rail
GND	Ground	Common Ground

Table 6.3: Pin Mapping Between ESP32, SX1276 and PE4259

The ESP32 controls the signal path by altering the logic state of the CTRL pin, effectively choosing whether RF1 or RF2 is connected to the common RF port. In our case, since only one antenna port and one transceiver port are used, the RF switch functions as a routing controller with a fixed mapping to ensure signal flow from the SX1276 to the antenna.

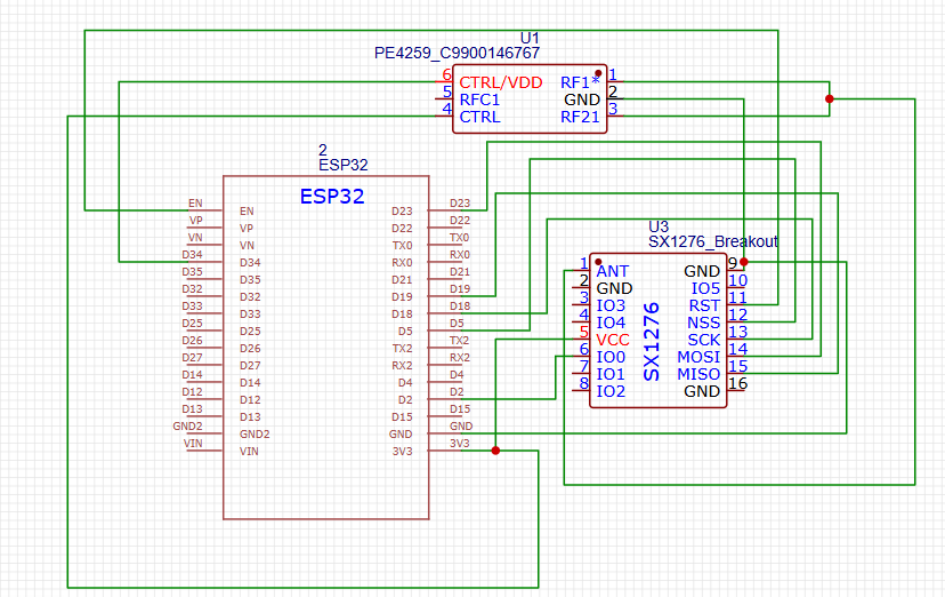

Figure 6.4: PE4259 RF Switch in the Transceiver System

6.4 Antenna Port Switching logic

In the design of a dual-band LoRa transceiver system, it is essential to ensure that the antenna can effectively operate at both 433 MHz and 870 MHz frequencies without requiring multiple antenna ports. To achieve this, a single-port microstrip antenna was designed with dual-band capability, and an RF switch was employed to route signals from the transceiver to the appropriate frequency path. The switching between these two frequency bands is controlled by the ESP32 microcontroller using a simple yet effective digital control method.

The RF switch used in this project is the PE4259, which offers low insertion loss, high isolation, and a fast response time. It has three RF ports: RF1, RF2, and RFC (common port). The two frequency feeds of the antenna are connected to RF1 and RF2, while the common RFC port is connected to the transceiver's RF output. The switch is controlled by a single digital logic signal, known as the CTRL pin. When the CTRL pin is set to logic LOW, RFC connects to RF1, enabling operation at 433 MHz. When set to logic HIGH, RFC connects to RF2, switching the antenna path to 870 MHz. This binary logic switching provides an elegant way to manage dual-band operation without physical intervention or multiple antennas.

The following code demonstrates this integration. It initializes the LoRa module, toggles the RF switch using ESP32 GPIO, and alternates operation between 433 MHz and 870 MHz bands every 10 seconds. This not only validates the switch's operation but also confirms the antenna's dual-band performance via software control.

```
#include <SPI.h>
#include <LoRa.h>
#define RF_SWITCH_CTRL  34
#define FREQ_433 433E6
#define FREQ_870 870E6
void setup() {
  Serial.begin(9600);
  delay(1000);
  pinMode(RF_SWITCH_CTRL, OUTPUT);
  // Initially select 433 MHz
  digitalWrite(RF_SWITCH_CTRL, LOW);
  Serial.println("Routing antenna to 433 MHz feed");
```

```
  if (!LoRa.begin(FREQ_433)) {
    Serial.println("LoRa initialization failed at 433 MHz!");
    while (1);
  }
  Serial.println("LoRa initialized at 433 MHz");
}
void loop() {
  // Wait 10 seconds then switch
  delay(10000);
  // Switch to 870 MHz
  digitalWrite(RF_SWITCH_CTRL, HIGH);
  LoRa.end();
  Serial.println("Routing antenna to 870 MHz feed");
  if (!LoRa.begin(FREQ_870)) {
    Serial.println("LoRa initialization failed at 870 MHz!");
    while (1);
  }
  Serial.println("LoRa initialized at 870 MHz");
  delay(10000);
  // Switch back to 433 MHz
  digitalWrite(RF_SWITCH_CTRL, LOW);
  LoRa.end();
  Serial.println("Routing antenna back to 433 MHz feed");
  if (!LoRa.begin(FREQ_433)) {
    Serial.println("LoRa initialization failed at 433 MHz!");
    while (1);
  }
  Serial.println("LoRa reinitialized at 433 MHz");
}
```

To better understand the implementation, a block-level schematic was created showing the ESP32 interfacing with both the PE4259 RF switch and the SX1276 LoRa module. The schematic illustrates GPIO 16 connected to the CTRL pin of the RF switch, while the RF1 and RF2 ports are routed to different feedlines of the antenna, and the RFC port connects to the transceiver's RF output. This arrangement allows the system to switch bands in real-time without reconfiguring the hardware.

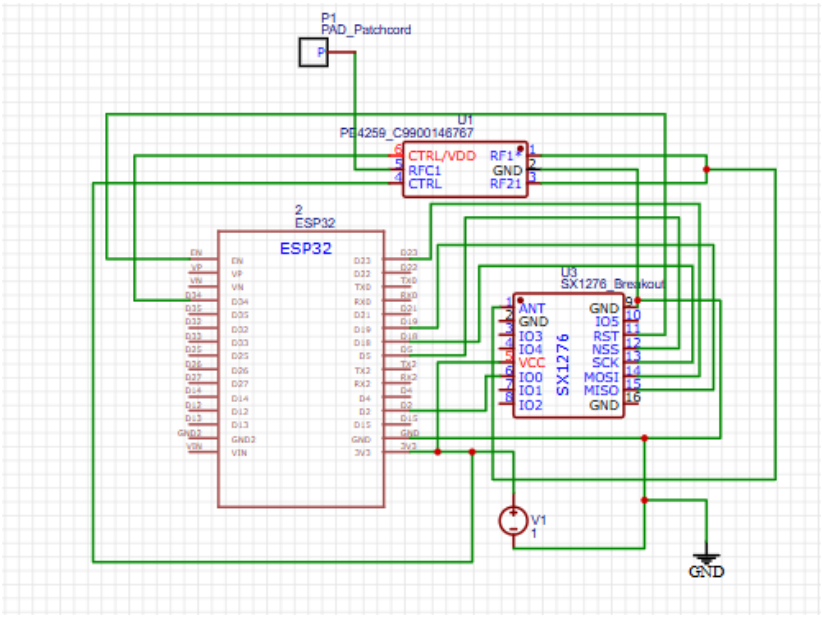

Figure 6.5: **Schematic diagram of LoRa Transceiver**

The flow of the control logic used in this design can also be described as follows: the system powers on and initializes the serial interface and LoRa transceiver. The ESP32 sets its GPIO pin to a defined logic level to select the desired band. Based on the GPIO state, the RF switch routes the signal path accordingly. The LoRa module is then initialized for the selected frequency. After a defined delay, the GPIO pin toggles, the switch re-routes the signal path, and the LoRa module is reinitialized for the new frequency. This cycle continues, allowing alternating communication across both bands.

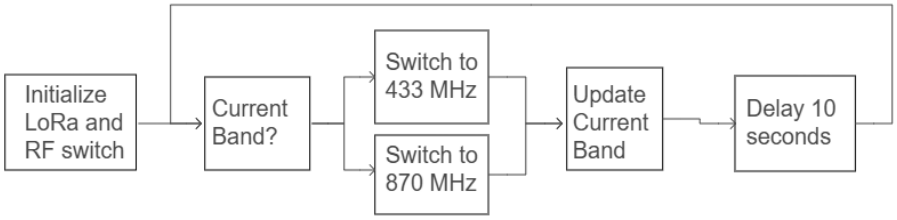

Figure 6.6 Antenna Switching Flowchart Using ESP32 and PE4259

This flowchart offers a clear and structured overview of the control logic that enables real-time switching between dual-band frequencies using software. It complements the Arduino code implementation and illustrates the logical flow from initialization through continuous switching cycles, which is crucial for validating the effectiveness of the single-port dual-band antenna design.

6.5 PCB Design

In the proposed LoRa transceiver system, a four-layer PCB architecture was adopted to ensure robust signal integrity, efficient power distribution, and minimal electromagnetic interference. The board measures approximately 58.29 mm × 57.4 mm, offering a compact layout that accommodates all essential components without compromising on performance. The top layer is dedicated to routing high-frequency RF signals and placing critical surface-mount components such as the SX1276 LoRa transceiver, the PE4259 RF switch, and the antenna feedline. This configuration helps minimize parasitic inductance and capacitive coupling by reducing trace lengths and allowing precise impedance control.

The first inner layer is implemented as a solid ground plane, serving as a continuous return path for RF signals and digital lines. This layer plays a vital role in shielding the signal traces from external noise and also supports proper signal referencing for controlled impedance design. Beneath this, the second inner layer functions as a dedicated 3.3V power plane, delivering regulated voltage to all active components while minimizing voltage drop and IR losses across the board. This layer helps to decouple noisy digital supply lines from sensitive analog and RF circuits.

The bottom layer is primarily used for digital routing and low-frequency control signals, such as the SPI interface and GPIOs from the ESP32 to the SX1276 and RF switch. The routing on this layer was carefully managed to maintain sufficient spacing from RF traces and avoid crosstalk or coupling that could degrade signal performance.

Routing width was maintained at 0.5 mm, and microstrip lines were modeled to provide a controlled 50-ohm impedance, particularly for the critical RF paths between the transceiver, switch, and antenna port. Special attention was given to the RF control line (CTRL) from the ESP32, which was routed on the bottom layer far from high-frequency paths to prevent digital switching noise from interfering with RF performance.The complete simulated PCB layout, including all four layers, is shown in the figures below.

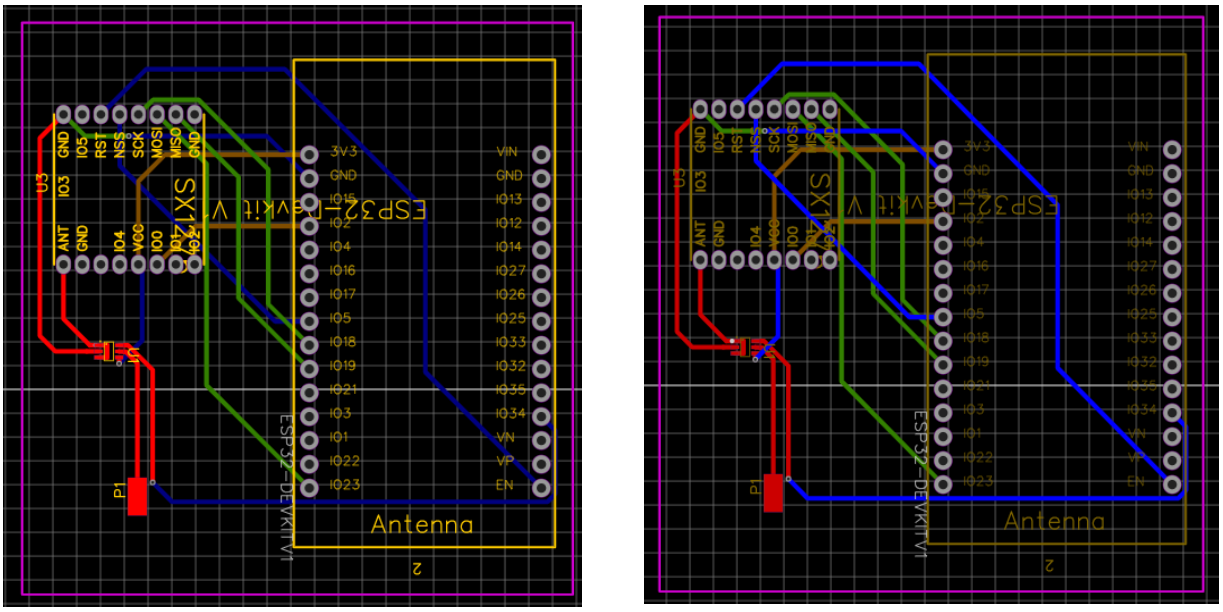

Figure 6.7: Top Layer and Bottom Layer Routing

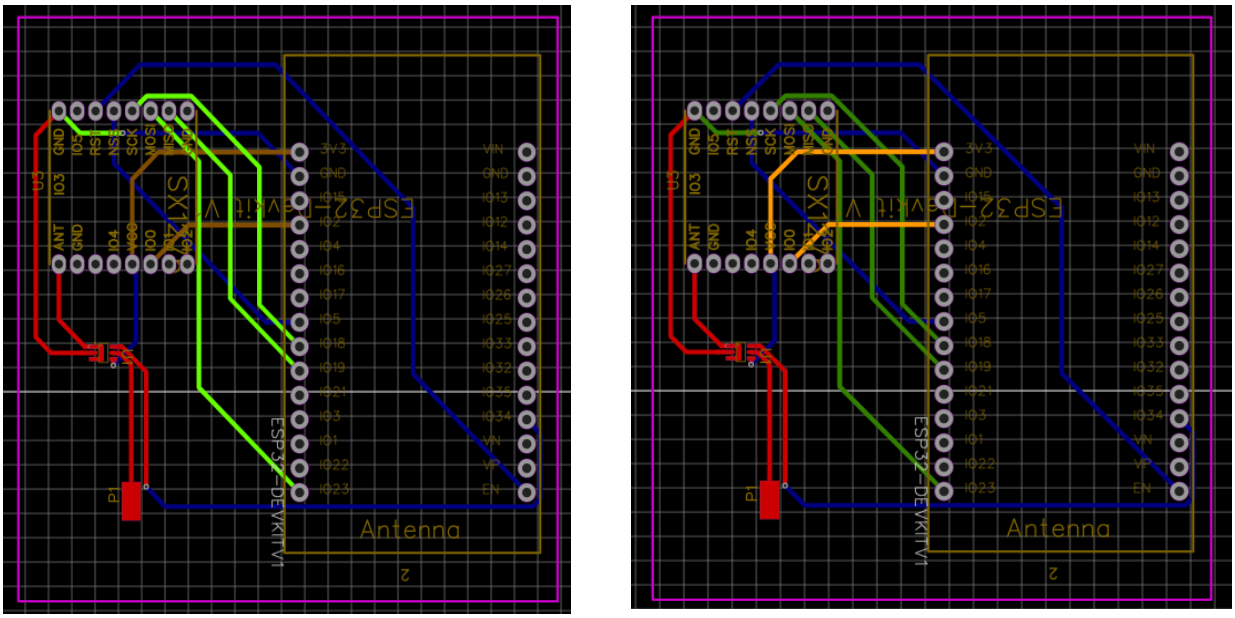

Figure 6.8: First and Second Inner Layer Routing

7

CONCLUSION & FUTURE SCOPE

7.1. Conclusion

This dissertation presented the design and development of a dual-band LoRa transceiver system aimed at enhancing wireless communication in Internet of Things (IoT) applications. A compact rectangular microstrip patch antenna was carefully engineered to resonate at two key ISM bands — 433 MHz and 870 MHz — enabling robust and flexible communication across a wider spectrum. The antenna achieved significant return loss values below –10 dB at both target frequencies, demonstrating its suitability for efficient signal transmission with minimal power loss.

To complement the antenna design, an integrated hardware system was developed featuring the SX1276 LoRa module and ESP32 microcontroller. A key innovation in the system was the incorporation of an RF switch (PE4259), allowing dynamic antenna port selection based on operating frequency, all controlled through GPIO logic from the ESP32. The interfacing between components was streamlined through a carefully designed 4-layer PCB, simulated and routed using software tools, optimizing trace width, impedance matching, and RF isolation.

The system simulation results, including S-parameters, gain plots, and radiation patterns, confirmed the effectiveness of the antenna and the overall integration strategy. While the hardware prototype was not fabricated, the complete system-level design provides a strong foundation for physical realization and deployment. The project demonstrates the viability of multi-band LoRa systems for scalable and flexible IoT networks, offering enhanced range and reliability.

7.2. Future Scope

- **Physical Fabrication and Testing**: The designed PCB and antenna can be fabricated to validate real-world performance. Parameters like VSWR, S11, gain, and radiation pattern can be measured using a VNA and anechoic chamber.

- **Multi-band Antenna Development**: The current dual-band antenna may be extended to a **tri-band or reconfigurable design** to support additional ISM bands like 2.4 GHz, improving global interoperability for LoRa and other wireless protocols.

- **Energy-Autonomous LoRa Nodes** The integration of **energy harvesting modules** (solar, thermal, or RF scavengers) with supercapacitors could lead to self-powered, maintenance-free LoRa nodes — ideal for deployment in hard-to-reach or hazardous environments.

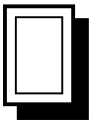

REFERENCES

[1] M. Bor, U. Roedig, T. Voigt, and J. M. Alonso, “Do LoRa low-power wide-area networks scale?” in *Proceedings of the 19th ACM International Conference on Modeling, Analysis and Simulation of Wireless and Mobile Systems*, 2016, pp. 59–67.

[2] F. Adelantado, X. Vilajosana, P. Tuset-Peiro, B. Martinez, J. Melia-Segui, and T. Watteyne, “Understanding the limits of LoRaWAN,” *IEEE Communications Magazine*, vol. 55, no. 9, pp. 34–40, 2017.

[3] M. Centenaro, L. Vangelista, A. Zanella, and M. Zorzi, “Long-range communications in unlicensed bands: The rising stars in the IoT and smart city scenarios,” *IEEE Wireless Communications*, vol. 23, no. 5, pp. 60–67, 2016.

[4] C. Ranaweera and C. Jayasundara, “Performance evaluation of antenna design for long-range IoT networks using LoRa,” *IEEE Internet of Things Journal*, vol. 7, no. 9, pp. 8422–8430, Sep. 2020.

[5] D. Bouchouicha, F. Bouabdallah, S. Boutayeb, and R. Taleb, “Energy consumption model for sensor nodes based on LoRa and LoRaWAN,” *Computer Communications*, vol. 128, pp. 198–203, 2018.

[6] H. T. Nguyen, T. H. Le, and Q. V. Tran, “A compact 433 MHz antenna design for LoRa applications in precision agriculture,” in *Proc. IEEE Int. Conf. on Advanced Technologies for Communications (ATC)*, pp. 111–115, 2020.

[7] M. A. Islam, M. T. Islam, and N. Misran, “Dual-band monopole antenna for LoRa-based IoT applications,” *IEEE Access*, vol. 8, pp. 146912–146920, 2020.

[8] S. Rajendran, N. Moayeri, and A. Ghasemi, “Evaluation of chip antenna performance in LoRa-based wireless sensor platforms,” *IEEE Sensors Journal*, vol. 19, no. 10, pp. 3713–3720, May 2019.

[9] T. Althobaiti et al., "A Compact Dipole Patch Antenna for RFID and IoT Applications," *IEEE Access*, 2022.

[10] M. E. Adejo, S. D. Walker, and K. A. A. Gamage, "Compact Dual Band Microstrip Patch Antenna for LoRa IoT Applications," *Proc. 2023 Int. Conf. Wireless Commun., SignalProcess.Netw.(WiSPNET)*,pp.1–5.

[11] A. Vamseekrishna et al., "Design of a Multi-Band Reconfigurable Antenna Using RT Duroid 5880 for Wireless and IoT Applications," *IEEE Trans. Antennas Propag.*, vol.2021.

[12] H. Raza, M. Rehman, and S. D. Zargar, "A review on RF switches for reconfigurable antenna systems," *IEEE Access*, vol. 7, pp. 146190–146202, 2019.

[13] Shixiang An , Hua Wang ,, “Time Domain Multiplexed LoRa Modulation Waveform Design for IoT Communication” IEEE COMMUNICATIONS LETTERS, VOL. 26, NO. 4, APRIL 2022.

[14] Nikola Jovalekic , Vujo Drndarevic,, “LoRa Transceiver With Improved Characteristics” IEEE WIRELESS COMMUNICATIONS LETTERS, VOL. 7, NO. 6, DECEMBER 2018.

[15] Muhammad Sani Yahya, Socheatra Soeung , Francis Emmanuel Chinda ,, “A Compact Dual Band Microstrip Patch Antenna for LoRa IoT Applications” IEEE OPEN JOURNAL OF ANTENNAS AND PROPAGATION,VOL.5,NO.4 AUGUST 2023

[16] Panagiotis Gkotsiopoulos, Dimitrios Zorbas,“Performance Determinants in LoRa Networks: A Literature Review” IEEE COMMUNICATIONS SURVEYS & TUTORIALS, VOL. 23, NO. 3, THIRD QUARTER 2021.

[17] Ali Waqar Azim , Jorge L. Gulfo Monsalv, “Enhanced PSK-LoRa” IEEE WIRELESS COMMUNICATIONS LETTERS, VOL. 11, NO. 3, MARCH 2022.

[18] SX1276 Datasheet.

[19] ESP32 Datasheet.

[20] PE4259 Datasheet